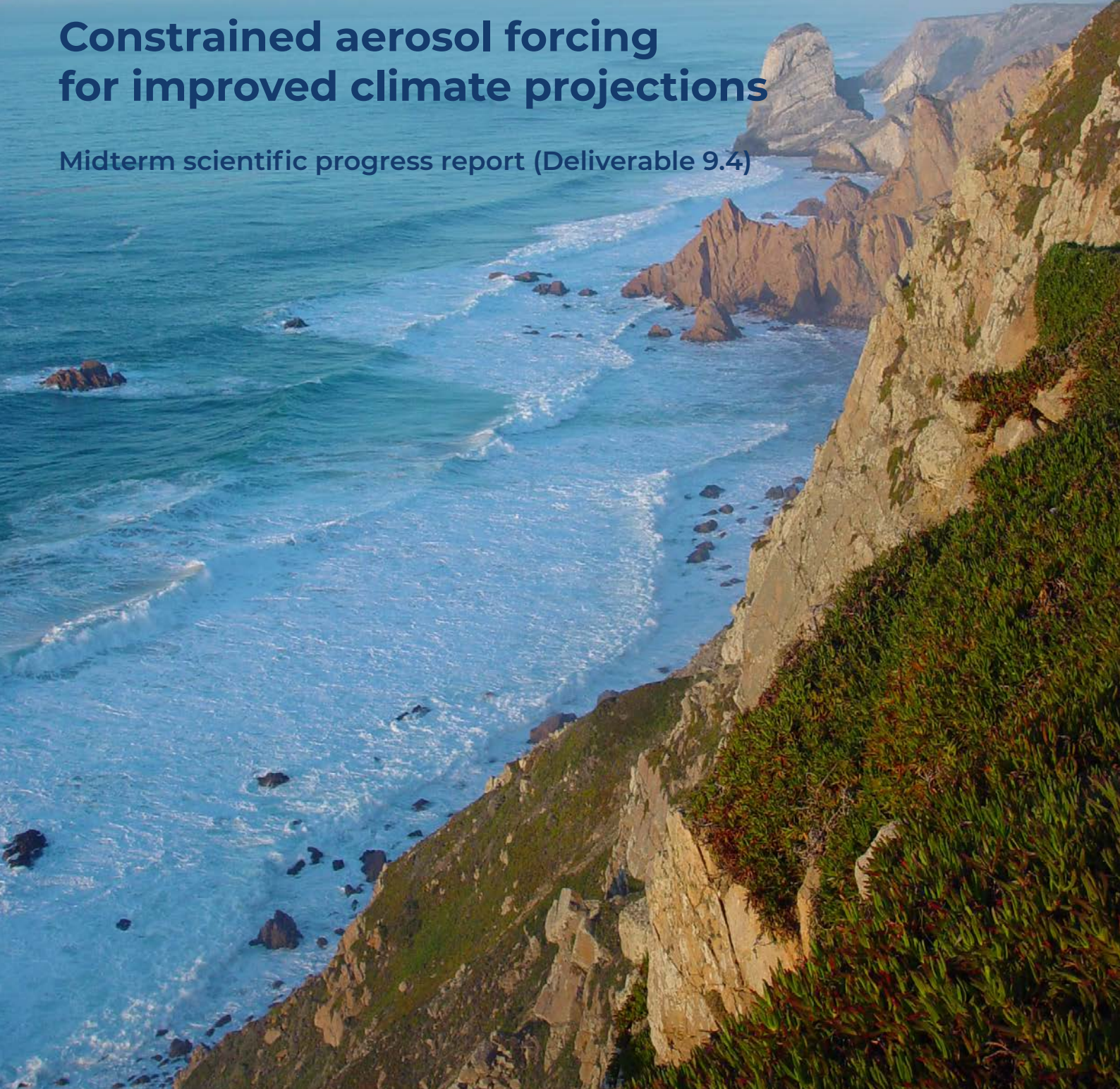


Constrained aerosol forcing for improved climate projections

Midterm scientific progress report (Deliverable 9.4)



The ultimate aim of the FORCeS project is to understand and reduce the long-standing uncertainty in anthropogenic aerosol radiative forcing. This is crucial if we are to increase confidence in climate projections.



This project has received funding from the European Union's Horizon 2020 research and innovation programme under grant agreement No 821205.

The contents of this document are the sole responsibility of the authors and do not reflect the opinion of the European Commission. The European Commission is not responsible for any use that may be made of the information contained in this document.

Copyright © FORCeS Consortium

Contents

1. Summary	3
2. Dissemination uptake	3
3. Background and FORCeS objectives	3
4. Approach and methods used within FORCeS science	4
5. Scientific outcomes and progress within the FORCeS WPs during the first two years of the project	6
5.1 Progress within WP1 “Critical aerosol forcing processes and factors”	6
5.2 Progress within WP2 “Understanding of cloud processes and aerosol-cloud interactions”	11
5.3 Progress within WP3 “Role of aerosol and cloud changes for aerosol radiative forcing between 1950 and 2050”	16
5.4 Progress within WP4 “Novel constraints on aerosol radiative effects”	20
5.5 Progress within WP5 “Climate response and feedbacks within ESMS”	24
5.6 Progress within WP6 “Constraining climate sensitivity and near-term climate response”	27
5.7 Scientific progress contributing to the FORCeS objectives during the first two years of the project	28
6. Summary and outlook	29
References	29
FORCeS contact information	34

Document information

Project title: FORCeS – Constrained aerosol forcing for improved climate projections

Grant Agreement 821205

Coordinator: Stockholm University (SU)

Coordinators: Ilona Riipinen (SU) and Annica Ekman (SU)

Document title: Deliverable 9.4 – Scientific progress report

Work package: WP9 – Scientific management

Contributing partners: All Partners

Lead authors: Ilona Riipinen (SU) and Annica Ekman (SU)

Contributing authors: FORCeS work package leaders

Submission date: 15.12.2021

1. Summary

This document summarizes the mid-term scientific progress of the European Union (EU) Horizon 2020 project FORCeS (“Constrained aerosol forcing for improved climate projections”). It is based on the original peer-reviewed literature associated with the work conducted within the project, covering 59 articles in international scientific journals and in addition some conference presentations. Overall, FORCeS has progressed according to the original plan, and the scientific progress made has helped the project progress towards its objectives and goal, as specified in this report. For further information on the project, please see forces-project.eu.

2. Dissemination uptake

This report is aimed at scientists, policymakers and the general interested public. However, it is in the form of a scientific report, so some scientific literacy and knowledge of the basic concepts within atmospheric and climate science is needed. It is based on the body of peer-reviewed literature, and just briefly highlights the topics covered and key results obtained within these 59 scientific articles. Detailed descriptions of the studies conducted, the methodologies used, the results obtained and the conclusions drawn can be found in these articles – the grand majority of which are freely and openly available online (see the References section).

3. Background and FORCeS objectives

The challenge: The Paris Agreement (PA), adopted within the United Nations Framework Convention on Climate Change (UNFCCC) in December 2015, requires the majority of the world’s countries to limit global warming from anthropogenic activities within 2°C above pre-industrial levels. The actions needed to reach this goal, and the urgency and effectiveness of their implementation, rely crucially on accurately predicting the time-evolution of radiative forcing and the resulting climate response. Uncertainty in simulating the components of the atmosphere, especially those related to aerosol, clouds and their interactions severely hampers our ability to understand the past and project future climate change. This is because anthropogenic aerosols exert a net cooling impact on climate that offsets – but with large uncertainty – part of the warming effect from greenhouse gas emissions. As a result, the time left for achieving the necessary greenhouse gas reductions to achieve the PA target, and our understanding of the expected regional impacts of climate change, are hampered by the inability to robustly quantify the anthropogenic climate forcing associated with aerosols. In particular, the anticipated large reductions in aerosol emissions in the coming decades will result in a warming effect that is currently very poorly quantified. It is therefore crucial to establish the extent to which aerosol changes, whether due to anthropogenic emissions or as a feedback induced by warming, offset greenhouse gas warming.

The goal of FORCeS is to resolve the above challenge and, in support of the Intergovernmental Panel on Climate Change (IPCC), substantially increase the confidence in estimates of aerosol radiative forcing and its impact on transient climate response. FORCeS will do this by bridging a crucial gap that currently exists between knowledge on the process scale and model application on the climate scale. FORCeS will identify, observationally constrain and efficiently parameterize the most important processes driving aerosol radiative forcing. With this knowledge, FORCeS will produce more robust estimates of the overall aerosol contribution to past climate change, leading to tighter constraints on climate sensitivity, and ultimately more accurate projections of the near-term climate change. Observations, computational models and theoretical considerations will be used to constrain and predict the anthropogenic aerosol impact on climate. A novel combination of computational and data mining techniques, brought together for the first time within FORCeS, will aid in establishing a good balance between an accurate representation of aerosol processes with computational requirements and need for simplification within climate models. FORCeS will operate on a continuum of temporal and spatial scales, focusing on metrics and outcomes with direct relevance for policy and ultimately for the quality of life. Based on the scientific knowledge gained, FORCeS will inform decision and policy makers about the effect of aerosol emission changes on regional and global climate evolution and on emission pathways to meet the targets of the PA.

To reach its goal, FORCeS will

- Identify the most important cloud and aerosol processes or components controlling radiative forcing and transient climate response. Make targeted improvements of the corresponding parameterizations for a set of leading European climate models, to obtain more reliable transient climate simulations. (**OBJECTIVE 1**).
- Exploit models, statistical methods, data mining and the recent wealth of observations to reduce the uncertainty in anthropogenic radiative forcing associated with aerosols and aerosol-cloud interactions from more than $\pm 100\%$ to closer to $\pm 50\%$. (**OBJECTIVE 2**).
- Quantify the near-term climate impact and associated uncertainty ranges for a set of plausible combinations of near-term greenhouse gas and aerosol emission pathways, in support of the Paris Agreement. (**OBJECTIVE 3**).

In the following Sections, we will describe the approach and methods used to reach, and the scientific progress towards, these Objectives.

4. Approach and methods used within FORCeS science

The key scientific bottlenecks that FORCeS targets, the scientific objectives (see Sect. 3) and the expected outcomes of FORCeS are schematically outlined in Fig. 1. FORCeS deals with a large breadth of processes and scales – all the way from building fundamental understanding on molecular-scale phenomena (nanometer

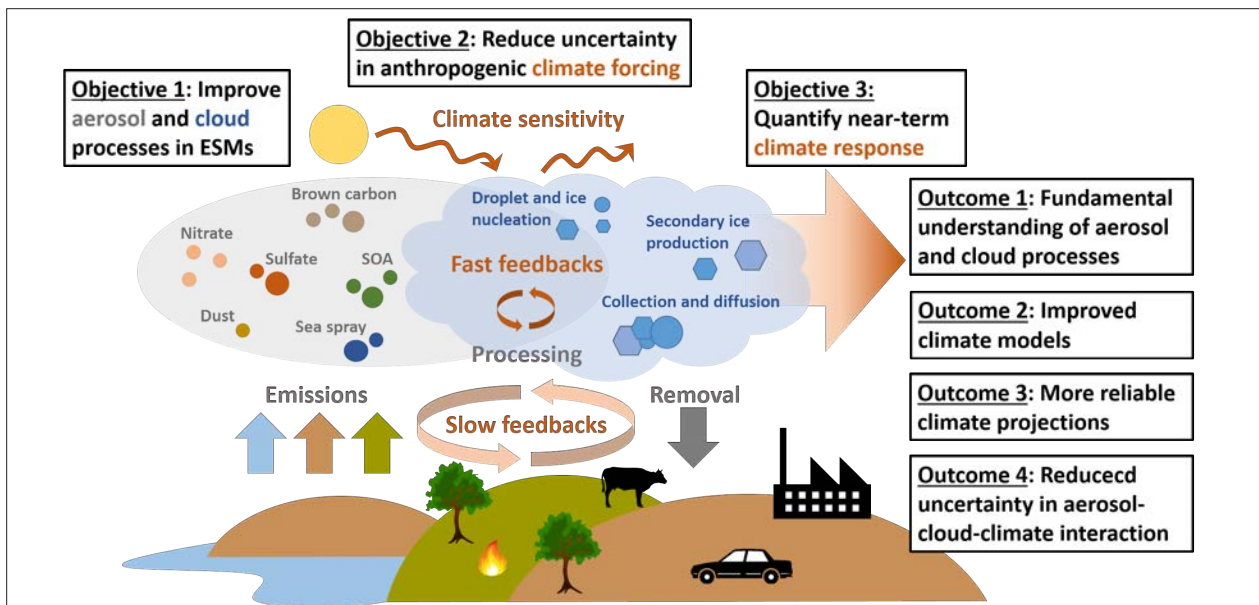


Figure 1. The knowledge gaps addressed in FORCeS, expected outcomes, and contribution to objectives. Figure by Tinja Olenius

scale) to understanding their implications on regional and global scales (scales from tens to several hundreds of kilometers). Therefore, the associated time scales also range from less than seconds up to centuries. This is an exciting scientific and methodological challenge to address.

The key for successfully addressing the challenge of bridging over spatial and temporal scales is the smart combination and connection of the relevant theoretical and experimental techniques applied within and outside the field of atmospheric and climate science (see Fig. 2). To succeed with the overall goals of the project (see Sect. 3), all process-level investigations within FORCeS will be guided by and conducted with the ultimate aim of improving the climate models used within FORCeS. The overall concept is based on the following three pillars, where particularly pillars I and II are relevant for this report:

Pillar I) Quantifying aerosol loadings and aerosol climate forcing through combining “bottom-up” process knowledge with “top-down” constraints;

Pillar II) Targeted investigation of fundamental phenomena, their systematic up-scaling and climate model improvement using novel techniques such as machine learning;

Pillar III) Active communication using metrics and approaches relevant for climate assessment groups and stakeholders.

The practical implementation of the work within FORCeS is structured in nine interlinked Work Packages (WPs, see Fig. 3). The scientific activities are primarily conducted within WPs 1-6, and hence the description of the scientific progress below has been structured according to these WPs and the Tasks within them.

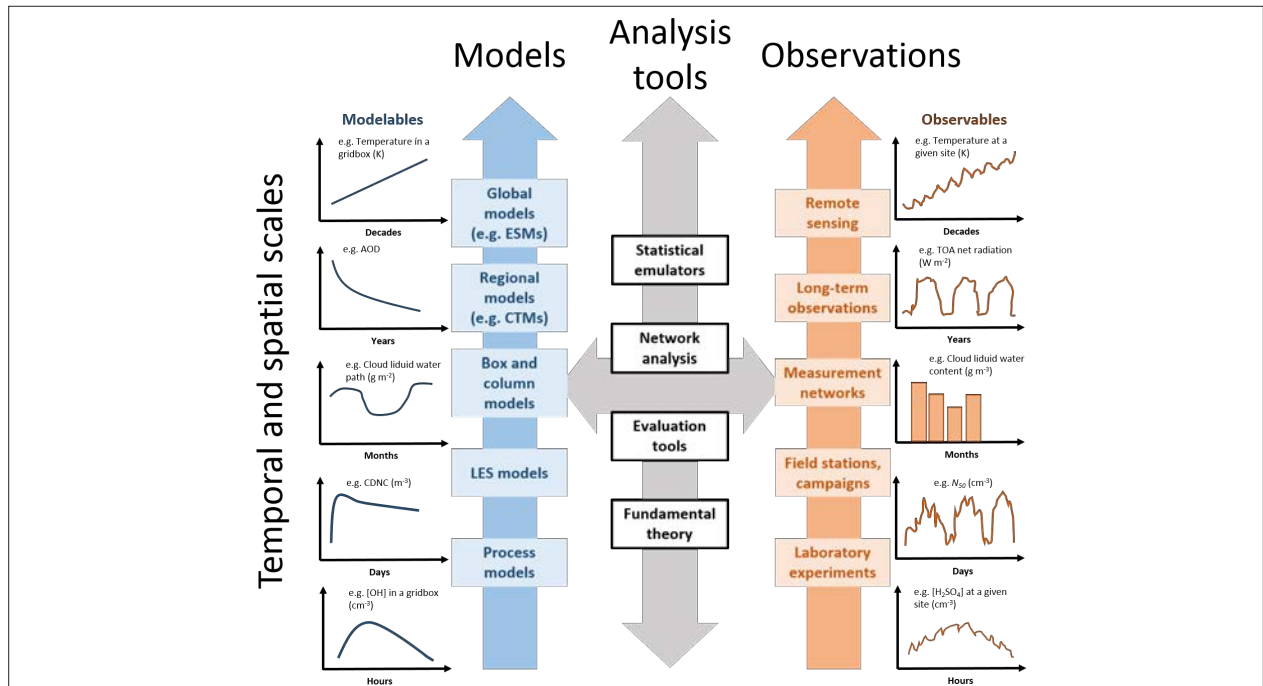


Figure 2. The relevant scales and methods applied in FORCeS for moving between them, along with examples of time series of key variables needed for quantifying the effective radiative forcing caused by aerosol particles and aerosol-cloud interactions (ER_{Fari+aci}). Figure by Tinja Olenius

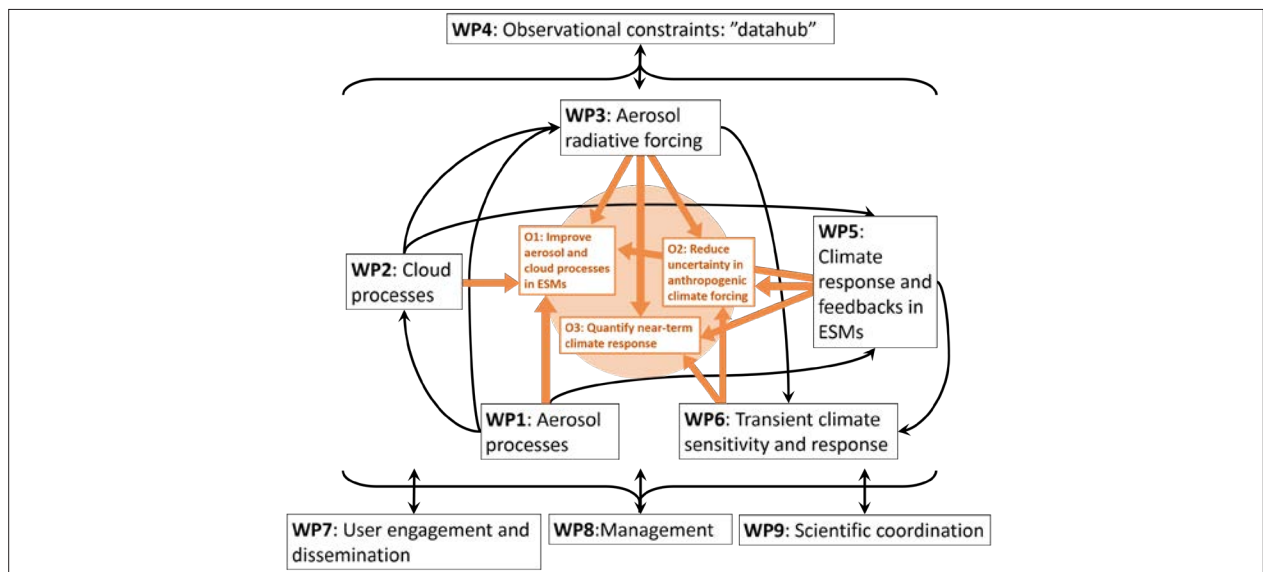


Figure 3. Graphical representation of FORCeS Work Package structure, their interactions (black arrows) and contribution to the overall objectives (see Sect. 3). Figure by Tinja Olenius

5. Scientific outcomes and progress within the FORCeS WPs during the first two years of the project

Overall, the work carried out in the first two years has progressed according to the plan within each of the scientific WPs 1–6 (see Fig. 3). As also envisioned in the Description of Action (DoA), the work within the different WPs is somewhat unevenly distributed in time between the different scientific WPs: while all Tasks within WPs 1–2 have been ongoing throughout the entire two-year period, this is not the case for WPs 3–6, where a large fraction of the Tasks has only just started or will start during the second half of the project. The significant progress achieved within WPs 1–2 provides important input for the other WPs, hence providing the basis for several of the Tasks within WPs 3–6 where intense efforts will be made now during the second half of the project. The scientific progress within WPs 1–6 is elaborated in detail below and the scientific progress towards the FORCeS objectives is summarized at the end of this Section.

5.1 Progress within WP1 “Critical aerosol forcing processes and factors”

The main objective of WP1 is the improvement of the representation of aerosol processes in the Earth System Models (ESMs) used within FORCeS (NorESM, EC-Earth, ECHAM-HAM) in an effort to increase the accuracy, and reduce the uncertainty, of the simulated aerosol effective radiative forcing (ERF). Based on recommendations of previous EU projects in this research area (particularly EUCAARI, PEGASOS, BACCHUS and ECLIPSE), and a series of dedicated FORCeS meetings, four key aerosol species and processes were selected for a deeper analysis: organic aerosol (OA), nitrate aerosol, brown carbon (BrC) and ultrafine aerosols.

During the first two years, the work in WP1 has progressed according to the DoA and focused on the development and initial testing of the first parameterizations related to the four key aerosol processes and components. The parameterizations developed here are being provided to WP3 and WP5 where they are included and tested in the FORCeS atmospheric general circulation models (AGCMs) and ESMs.

Task 1.1: Organic aerosol formation and chemical evolution

FORCeS is developing a reduced-form version of the complete ORACLE module developed by Tsimpidi et al. (2014), which is currently being tested within the FORCeS models. The module is based on the volatility basis set (VBS) framework proposed by Donahue et al. (2006). It uses fixed logarithmically-spaced saturation concentration bins to describe the OA volatility distribution and assumes formation of pseudo-ideal solutions in the organic aerosol phase. This framework blurs the distinction between the traditional primary (POA) and secondary organic aerosol (SOA), providing a more realistic picture of the behavior of atmospheric organic aerosol (see also Theodoritsi et al. 2021 for an application of the VBS scheme). The module simulates the gas-phase photochemical reactions of SOA precursors, and distributes the OA in the size modes used by the ESM. The parameters in this module can be easily updated by the latest laboratory findings regarding the formation of SOA, including detailed studies on the molecular evolution and volatility distributions of OA that are ongoing in the SAPHIRE chamber (see e.g. Wu et al., 2021 for such studies from FORCeS) and the field observations collected and analysed within the framework of FORCeS (e.g. Pasquier et al., 2021; Siegel et al., 2021 for such studies from FORCeS).

The laboratory studies on OA formation have targeted particularly the SOA formation through oxidation of various biogenic precursors by the NO₃ radical (Wu et al., 2021a, b; Bell et al., 2021), quantifying yields and volatility distributions of the formed aerosol (see Fig. 3 for an example from Wu et al., 2021a).

As an example from the field observations, the result of applying the FIGAERO-CIMS setup for analysing samples collected in the Arctic for the first time (see Siegel et al., 2021) reveals a potentially significant signal from organic and sulfur-containing compounds in the aerosol particles. These signals are indicative of marine aerosol sources, with a wide range of carbon numbers and O:C ratios – including a clear secondary component (see Fig. 5 from Siegel et al., 2021). Several of the sulfur-containing compounds were oxidation products of dimethyl sulfide (DMS), a gas released by phytoplankton and ice algae. These results highlight the importance of understanding the marine organics and DMS as a source of Cloud Condensation Nuclei (CCN) in this vulnerable region (see also Schmale et al., 2021 and references therein).

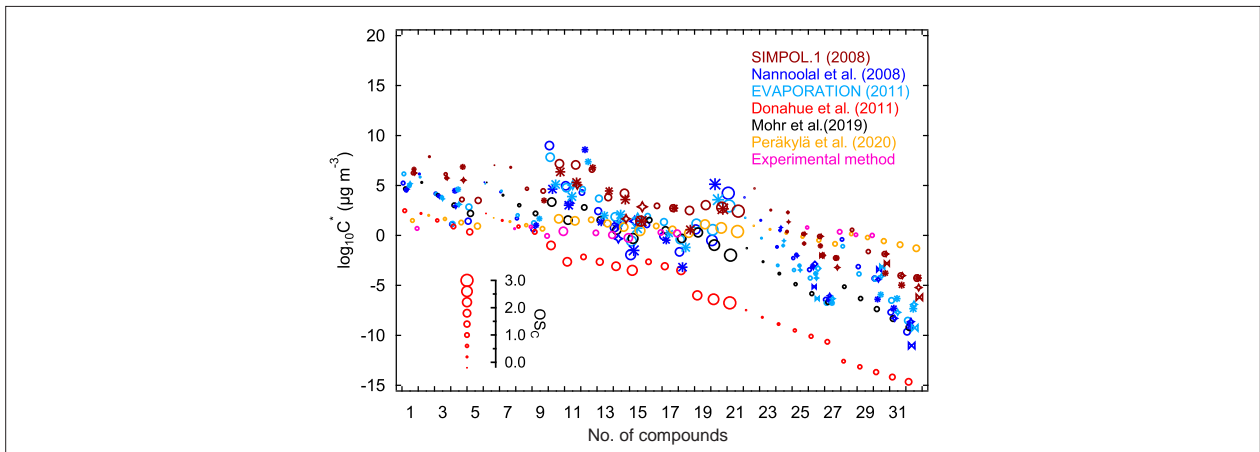


Figure 4. Figure from Wu et al. (2021a) comparing different approaches for determining saturation concentrations of oxidation products generated in the isoprene + NO₃ system. Saturation concentrations (in $\mu\text{g m}^{-3}$, at 298.15 K) of isoprene organonitrates estimated by using experimental and parameterization methods. The numbers correspond with the compound numbers of given in Table S2 within Wu et al., (2021a) (nos. 1–9, 10–18, 19–21, 22–27, and 28–32 corresponding to 1N-monomers, 2N-monomers, 3N-monomers, 2N-dimers, and 3N-dimers, respectively). Markers shapes indicate different isomers, with their size scaled by carbon oxidation state (OSC). Reproduced under the Creative Commons 4.0 (CC 4.0) license.

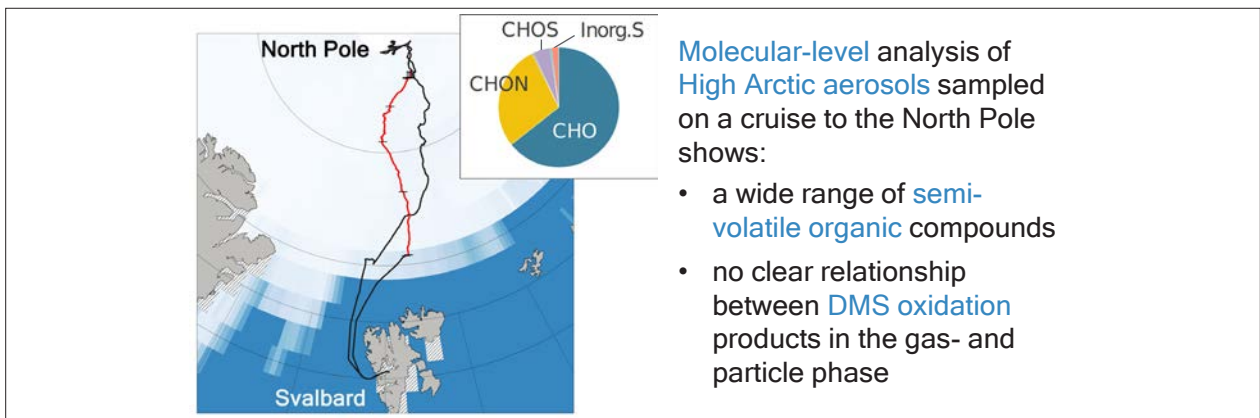


Figure 5. Adopted from Siegel et al. (2021), which illustrates the route of the MOCCHA cruise where aerosol samples were collected, along with a representative chemical composition of the samples and the key conclusions highlighted. Reproduced under the Creative Commons 3.0 (CC 3.0) license.

Another aspect of organic aerosol evolution and fate receiving special attention within FORCeS is the wet removal of OA and its precursors by clouds and precipitation (see also Sect. 5.2), given its important role in the overall OA budgets (see e.g. Holopainen et al., 2020). To investigate this process, Bardakov et al. (2021) used a framework coupling trajectories from a Large Eddy Simulation (LES) model MIMICA and a box model to investigate the uptake of isoprene and its oxidation products onto the hydrometeors within convective clouds in the tropical atmosphere (see Sect. 5.2 for more details).

Task 1.2: Nitrates in fine and coarse particles

Even if our understanding of the formation of inorganic nitrate salts has advanced and the corresponding processes are reasonably well simulated in regional chemical transport models (CTMs), the computational cost has seriously limited, and in most cases prohibited, the simulation of this aerosol component in ESMs. Besides influencing the radiative forcing caused by the aerosol particles, it is a key player in the atmospheric acid-base chemistry, which has important implications also for air quality and deposition of nutrients as demonstrated by a series of FORCeS-publications (Nenes et al., 2021; Kakavas and Pandis, 2021; Karydis et al., 2021; Baker et al., 2021; Paglione et al., 2021 see Fig. 6 for an example of the processes studied by Nenes et al., 2021).

Given the importance of simulating aerosol nitrate and acid-base chemistry accurately, we have in FORCeS explored ways to reduce the computational cost of the simulation of the formation and evaporation of ammonium nitrate, reactions of nitric acid with coarse sea-salt and dust particles, and the competition of fine and coarse particles for the available nitric acid. This has resulted in the development of ISORROPIA-lite, which is a simplified and computationally more efficient version of the thermodynamic model ISORROPIA-II (Fountoukis and Nenes 2007; Nenes et al., 2021; Karydis et al., 2021) that can be used by ESMs with a small additional computational cost to simulate aerosol nitrates. This is a very timely contribution, as the simulation of aerosol nitrate is still at a development stage in the FORCeS ESMs within WP5. The evaluation of ISORROPIA-lite is ongoing within FORCeS and the first results are promising as they show good agreement with ISORROPIA-II.

Minerals present in dust, such as calcite, influence aerosol pH and thus the distribution of nitrate between the gas and particulate phases (see e.g. Karydis et al., 2021). ESMs typically assume a globally uniform dust composition. Within FORCeS, a new climatology of dust is being developed. It will be used by the FORCeS ESMs, allowing them to characterize regional changes in dust composition and its potential impact on aerosol pH and nitrate (see e.g. Myriokefalitakis et al., 2021). The development relies on simulations done with the Multiscale Online Nonhydrostatic Atmosphere Chemistry (MONARCH) model (introduced by Pérez et al., 2011 and further developed within FORCeS by Klose et al., 2021). The brittle fragmentation theory (Kok et al., 2011) has been applied to represent the size-resolved fractional dust mineralogy at emission in MONARCH, following Perlwitz et al. (2015a, 2015b). MONARCH describes the size distribution through a sectional approach, considering 8 bins per mineral from 0.2 to 20 μm in diameter. The underlying soil composition information has been taken from two different sources: Claquin et al. (1999), with the modifications included by Nickovic et al. (2012), and Journet et al. (2014), which will ultimately provide a measure of mineral composition uncertainties and allow assessment of the sensitivity of ESMs to changes in mineral fractions. With these assumptions, MONARCH has been shown to be able to reproduce key features of the spatiotemporal variability of the global dust cycle (Klose et al., 2021, see Figs. 7 and 8).

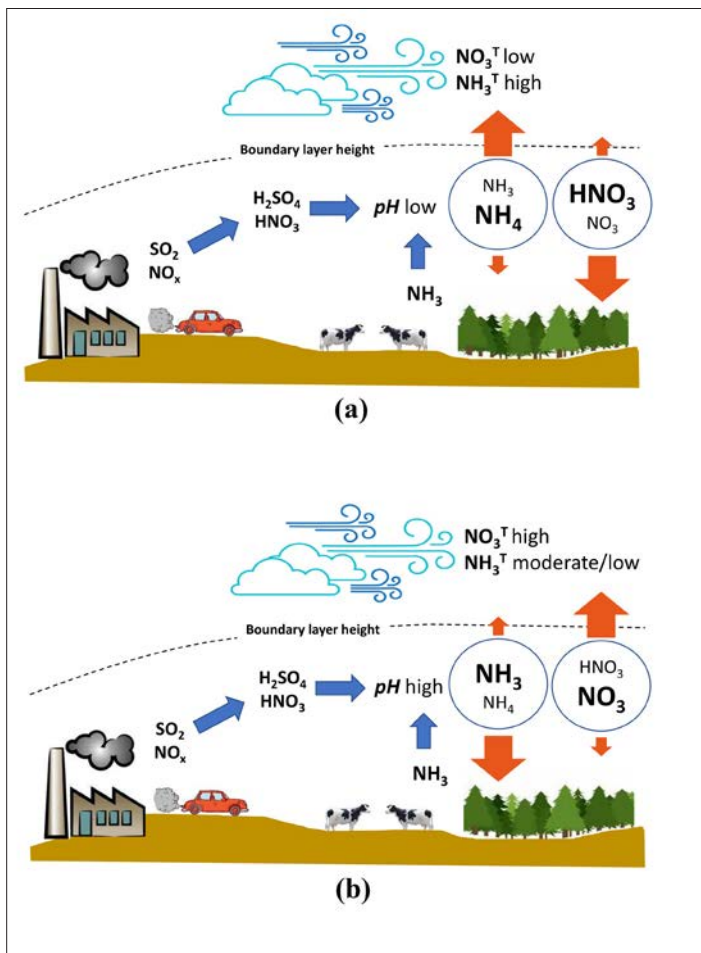


Figure 6. Summary sketch of the interactions between aerosol pH and emissions of total ammonium and nitrate from Nenes et al., 2021. (a) Aerosol pH is low and liquid water content is moderate, as is characteristic of the SE United States. Here the partitioning of ammonium is mostly in the aerosol phase, and the relevant dry deposition velocity is low. The concentration of total ammonium is dictated by the aerosol deposition velocity limit; ammonia export to the free troposphere is favored and vice versa for total nitrate. (b) Aerosol pH is high and liquid water content is moderate (as is characteristic of northern Europe in the winter and China). Here the partitioning of total ammonia is shifted to the gas phase, and the relevant dry deposition velocity is rapid. Total ammonia does not accumulate considerably in the boundary layer, and export to the free troposphere is minimal. Nitrate partitions to the aerosol phase, deposits slowly, and accumulates rapidly in the boundary layer. These conditions favor haze events and nitrate export to the free troposphere. Reproduced under the Creative Commons 4.0 (CC 4.0) license.

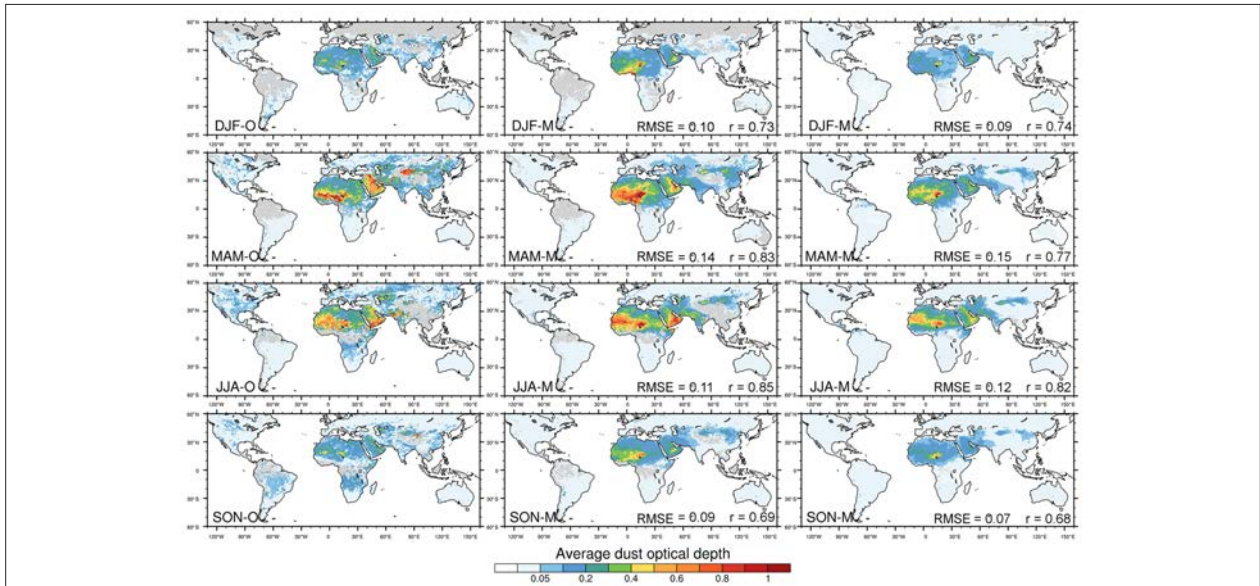


Figure 7. Seasonally averaged MODIS Deep Blue satellite Dust Optical Depth (DOD, left), MONARCH all-sky DODcoarse at satellite overpass times co-located with MODIS DOD (middle), and clear-sky DODcoarse at approximate satellite overpass times derived from 3-hourly model output from MONARCH (right). The model results were obtained for DODcoarse averaged across four model experiments. The seasonal averages were calculated with respect to the number of valid values per grid cell in the respective products. Area-weighted root mean square error (RMSE) and uncentered Pearson product-moment coefficient of linear correlation (r) between model and observations are indicated in the respective panels. Adopted from Klose et al. (2021). Reproduced under the Creative Commons 4.0 (CC 4.0) license.

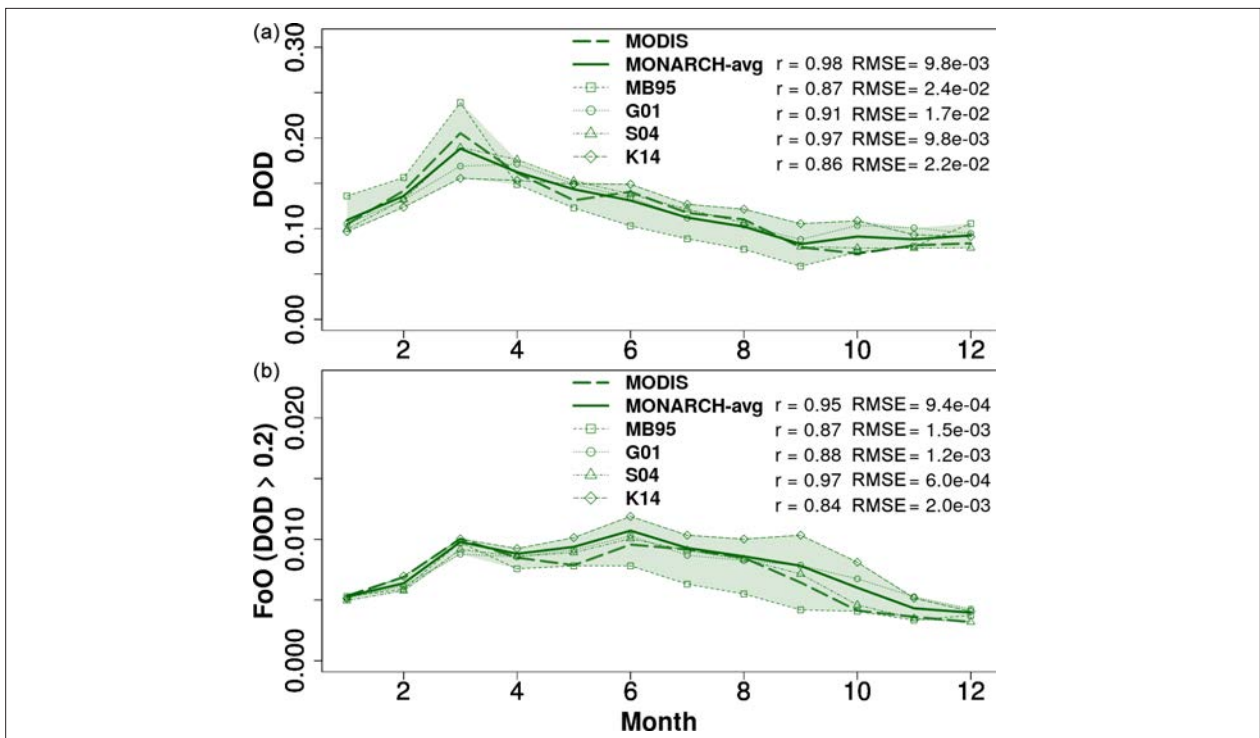


Figure 8. Globally averaged monthly global DODcoarse (a) and FoO of DOD > 0.2 (b) for MODIS (dashed green line) and MONARCH (DODcoarse all-sky co-located with MODIS observations) (green solid line). The shading indicates the range of DODcoarse across the four MONARCH experiments, which are also shown. Pearson correlation coefficients (r) and RMSE are given in the figure for both the experimental average as well as the individual runs. Adopted from Klose et al. (2021). Reproduced under the Creative Commons 4.0 (CC 4.0) license.

Task 1.3: Improved parameterizations of aerosol absorption

Three major types of aerosols have absorbing properties: black carbon (BC), brown carbon (BrC) and dust aerosols. BC is the type of aerosol that has the largest potential to warm the climate and it is currently considered in most climate models, including ESMs. Dust aerosol is partially absorbing. This is translated into dust aerosol having an imaginary part in its refractive index used in climate models. Dust aerosol is a mixture of different minerals, whose relative abundances, particle size distribution, shape, surface topography and mixing state influence their effect on climate. However, ESMs typically assume that dust is a homogeneous aerosol species, neglecting the known regional variations in the mineralogical composition of the sources. As described above (Task 1.2), a climatology considering the regional variation in the mineralogical composition of dust is being developed within FORCeS (see Kok et al., 2021a,b; Klose et al., 2021; Li et al., 2021) and will be implemented in FORCeS models. The work by Li et al. (2021) highlights particularly the need for an improved description of iron oxides (such as hematite and goethite) for capturing the radiative effects of dust.

While BC and dust are explicitly treated in most ESMs, BrC, which is the absorbing fraction of OA, is still disregarded by most climate models. This is despite its known impact on the effective radiative forcing due to aerosol-radiation-interactions (ERFari) and its potential impact on the snow albedo which may accelerate the melting of polar and glacial ice, similar to BC. Only recently has BrC attracted enough attention to start being incorporated in global climate models. Current climate models generally underestimate the absorbing properties of atmospheric aerosol although they reasonably estimate BC. As part of the AeroCom Phase III intercomparison of absorbing aerosol, Sand et al. (2021) evaluated the fraction of absorbing aerosol optical depth due to BC, dust, and organic aerosol and found it to be 57%, 30 and 10%, respectively (see also Figs. 9 and 10 for a comparison of the per-species mass absorption coefficients from Sand et al., 2021 illustrating the relative strength and contribution of each of these absorbing components).

The scientific work ongoing within FORCeS focuses particularly on how to further improve the estimates of dust (see e.g. Kok et al., 2021a, b; Kakavas and Pandis 2021) and BrC sources (related to e.g. biomass burning, see e.g. Theodoritsi et al., 2020) and absorption in the models (e.g. Frey et al., 2010; Sand et al., 2021).

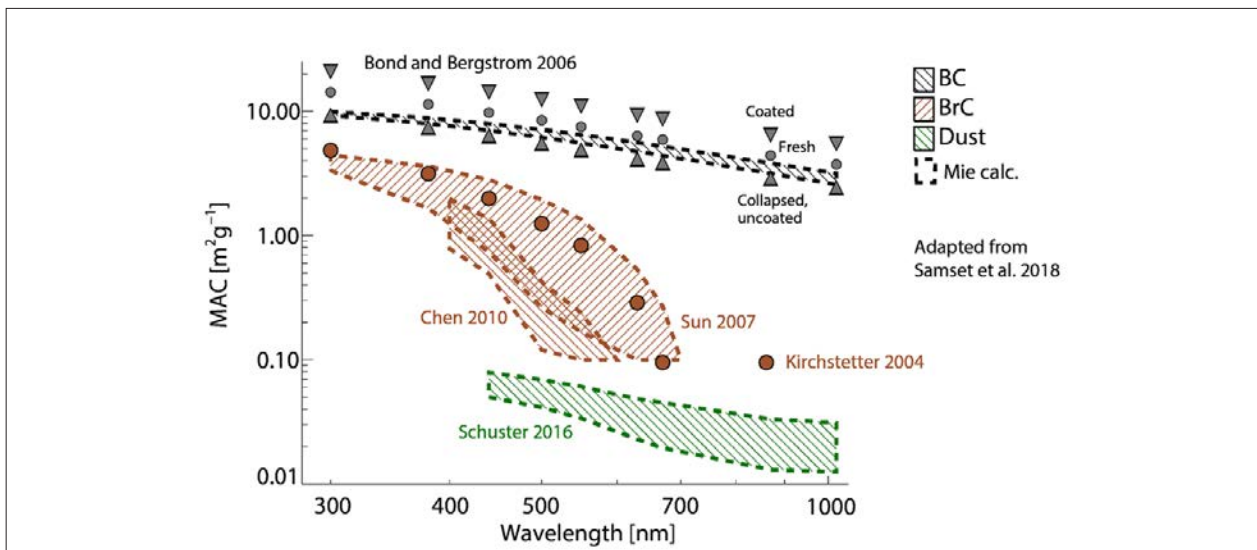


Figure 9. Per-species mass absorption coefficient (MAC) as a function of wavelength from observations and radiative transfer calculations. BC, BrC, and dust can be seen to have separable properties, which underlie the usage of these species as emitted, transported, and radiatively active particle types in most global climate models. Size distributions for BC and BrC had a radius and sigma of 0.04 μm and 1.5 for BC and 0.05 μm and 2.0 for BrC, while, for mineral dust, they used observed sizes from the DABEX aerosol campaign (Osborne et al., 2008). Aerosol densities were 1.2, 1.8, and 2.6 g cm^{-3} , for BrC, BC, and dust, respectively. Grey circles (triangles) illustrate MAC values for fresh (coated and uncoated) BC, where the Mie calculations have been scaled to achieve the recommended MAC of 7.5 $\text{m}^2 \text{g}^{-1}$ at 550 nm (Bond and Bergstrom, 2006). Adapted from Sand et al. (2021). Reproduced under the Creative Commons 4.0 (CC 4.0) license.

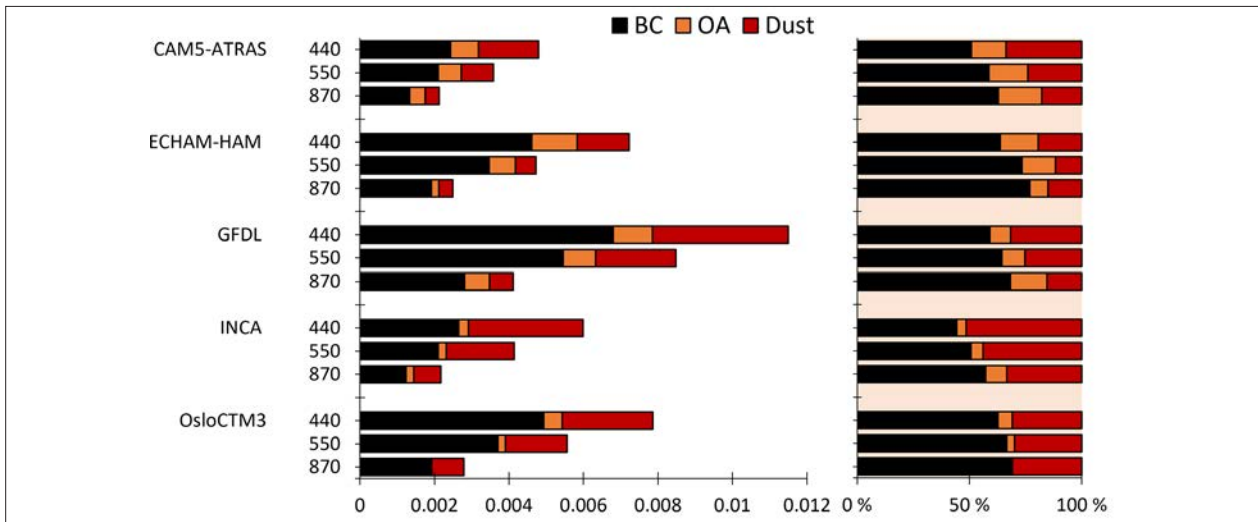


Figure 10. Global mean absorption aerosol optical depth (AAOD) at $\lambda=440, 550,$ and 870 nm for each model split into BC (black), OA (orange), and dust (red), with absolute values on the left and relative values on the right. Adapted from Sand et al. (2021). Reproduced under the Creative Commons 4.0 (CC 4.0) license.

Task 1.4: Ultrafine aerosol formation and growth

There are several ongoing efforts (but not yet published) in FORCeS to improve the parameterizations currently used in ESMs for the simulation of the ultrafine particles and the corresponding aerosol number distribution. The work has been focused on the improvement of the simulation of the new particle formation/growth processes based on both laboratory and field observations as well as on the treatment of number emissions. Our objective is once more to improve accuracy with a small computational cost for the ESMs.

Task 1.5: Identification of microphysical processes related to aerosols that can be simplified

The goal of this Task is the identification of microphysics processes related to aerosols to which the global models are less sensitive. The emphasis of this work is on aerosol-cloud interactions and cloud microphysical processes. The work conducted during the first two years (but not yet published) has focused particularly on microphysical processes related to aerosol formation and growth, and ice hydrometeors.

5.2 Progress within WP2 “Understanding of cloud processes and aerosol-cloud interactions”

The work within WP2 aims at an improvement of cloud-, precipitation and aerosol processes within ESMs, targeting particularly the processes governing the effective radiative forcing caused by aerosol-cloud interactions (ERF_{aci}). WP2 focuses on aerosol-cloud interactions and cloud microphysics and interacts particularly closely with WPs 3 and 5 through providing input and recommendations for the ESMs used within these WPs, and complements the aerosol process-focused WP1. Overall, the work within WP2 has progressed as outlined within the DoA. Many of the Tasks within WP2 are highly interlinked (see below for detailed descriptions).

Two major campaigns, one at Ny Ålesund station in the Arctic (NASCENT campaign coordinated by Stockholm University, from fall 2020 onwards, see Pasquier et al., 2021) and another at Puijo SMEAR IV station at the semi-urban environment (coordinated by the University of Eastern Finland, during fall 2021, see e.g. Väisänen et al., 2020; Ruuskanen et al., 2021) were planned and performed during the first two years, and the third campaign at the San Pietro Capofiume in Italy (coordinated by the National Research Council, Institute of Atmospheric Sciences and Climate (CNR-ISAC), see e.g. Paglione et al., 2021) is currently ongoing.

Task 2.1: Droplet activation

Recent results investigating links between aerosols and cloud microphysics from satellite data have demonstrated that the simple approaches typically used to derive the relationship between CDNC and aerosol particles

from observations of Aerosol Optical Depth (AOD) or Aerosol Index (AI) strongly underestimate the sensitivity, and that more elaborate ways to quantify the CCN concentration are required (Fig. 11, from Hasekamp et al., 2019).

Furthermore, a review with inputs from several FORCeS partners on the options to constrain the droplet activation from satellite observations has been conducted and published (Quaas et al. 2020). This review pointed out the general need to improve satellite-based methods to derive aerosol-cloud relationships. It emphasized the need to use Large Eddy Simulation (LES) to better assess the data requirements for CCN, updraft and cloud droplet number (N_d) observations, and to analyse the impact of spatial aggregation scales (see Fig. 12).

Furthermore, FORCeS is conducting LES studies that couple cloud activation to the other relevant processes that simultaneously take place when a cloud is formed. As an example, a study on the factors controlling Arctic cloud sustenance reveals the important role of Aitken mode particles in cloud droplet activation and cloud droplet number concentrations, hence highlighting the need for understanding the sources and sinks of these nanoscale particles in the Arctic (see Fig. 13 from Bulatovic et al. 2021; see also Schmale et al., 2020; Siegel et al., 2021; Maahn et al., 2021).

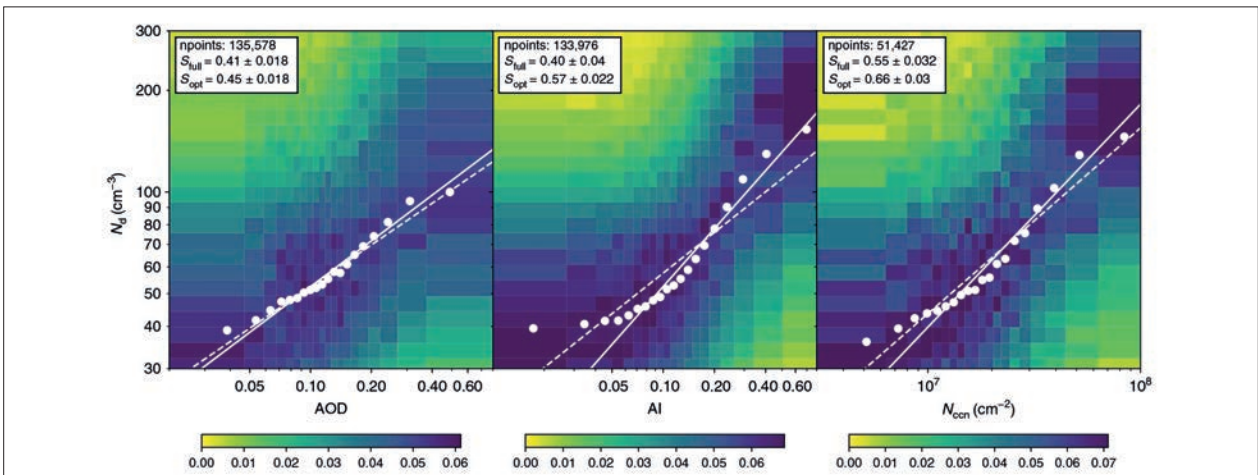


Figure 11. Dependence of cloud droplet number concentration on aerosol. Cloud droplet number concentration (N_d) versus aerosol optical depth (AOD), aerosol index (AI), and cloud condensation nuclei (CCN) column number (N_{ccn}), for the global ocean data set for 2006. Each point represents a bin median of N_d and CCN proxy, where each bin contains the same number of points (n points/20). The colors indicate the normalized histogram of N_d in each AOD/AI/ N_{ccn} -bin. The dashed lines show the linear regression through all data points and the solid lines using only data points for $N_{ccn} > 10^7 \text{ cm}^{-2}$, $\text{AI} > 0.05$, and $\text{AOD} > 0.07$, leaving out the lowest 15% of data for all 3 proxies. The quoted errors on the regression slope. Adopted from Hasekamp et al., 2019. Reproduced under Creative Commons 4.0 (CC 4.0) license.

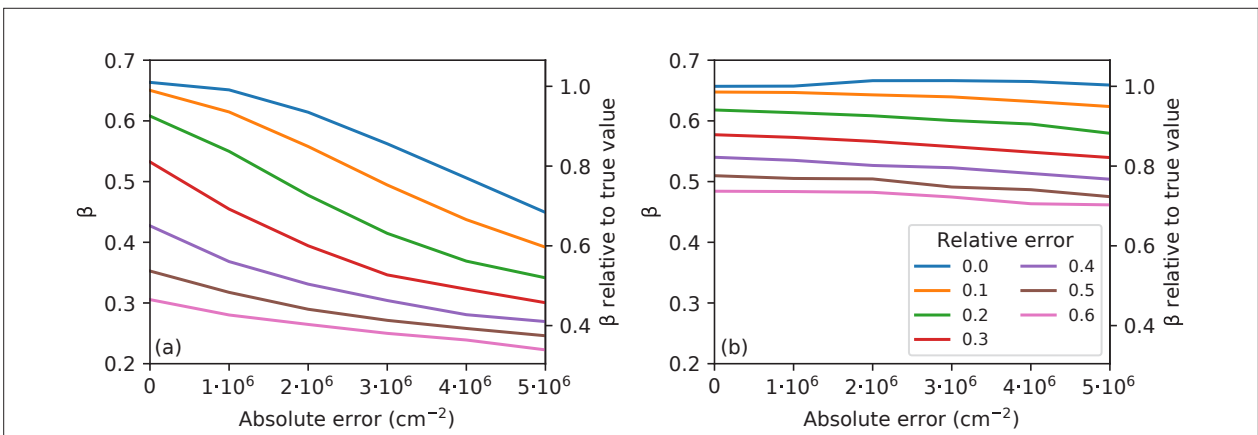


Figure 12. The sensitivity of N_d to CCN in the atmospheric column (β) as a function of the stochastic error in column CCN (absolute additive error) in an emulated analysis for the full range of data (a) and for the case when values of $N_{ccn} < 10^7 \text{ cm}^{-2}$ are excluded. Figure from Quaas et al. 2020. Reproduced under Creative Commons 4.0 (CC 4.0) license.

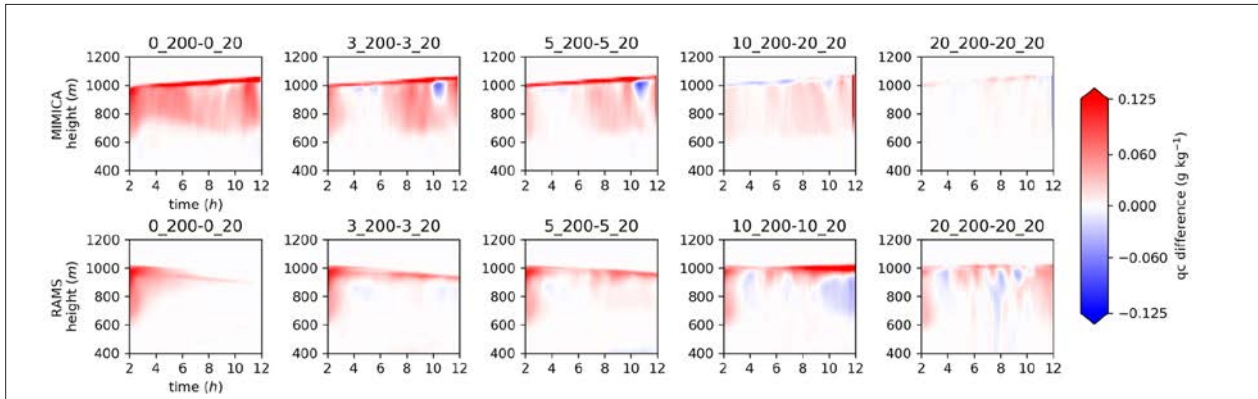


Figure 13. The influence of the varying Aitken mode particle concentrations on cloud droplet mixing ratios of simulations. The plots show differences in cloud droplet mixing ratios for Aitken mode concentrations of 200 vs. 20 cm^{-3} for a given accumulation mode concentration (from left to right 0, 3, 5, 10, or 20 cm^{-3}). Simulations run with 2 different LES models (MIMICA on the top row and RAMS on the bottom row). Figure from Bulatovic et al. (2021). Reproduced under Creative Commons 4.0 (CC 4.0) license.

On the detailed process level, the work conducted so far within FORCeS on the CCN activation aerosol particles has focused in particular on the CCN activation of BC (Laaksonen et al., 2020; Lohmann et al., 2020), which has traditionally been considered non-hygroscopic and does not participate in CCN activation in many global models. Laaksonen et al. (2020) present a theory describing heterogeneous nucleation on soot particles with adsorption nucleation theory, and conclude that soot particles can activate as CCN, and any treatment (including chemical ageing) that increases the number of adsorption sites will respectively increase their CCN activity. Lohmann et al. (2020), on the other hand, used ECHAM-HAM to conduct global simulations of past and future climate effects of both ozone-aged soot particles acting as cloud condensation nuclei and sulfuric acid-aged soot particles acting as ice-nucleating particles, and analysed the effects on structure and radiative effects of clouds (see Fig. 14 for a schematic of the studied processes). Under pre-industrial conditions, soot aging led to an increase in thick, low-level clouds that reduced negative shortwave effective radiative forcing by 0.2 to 0.3 W m^{-2} . In the simulations of a future, warmer climate under double pre-industrial atmospheric carbon dioxide concentrations, soot aging and compensating cloud adjustments led to a reduction in low-level clouds and enhanced high-altitude cirrus cloud thickness, which influenced the longwave radiative balance and exacerbated the global mean surface warming by 0.4 to 0.5 K. These findings suggest that reducing emissions of soot particles is beneficial for future climate, in addition to air quality and human health.

Task 2.2: Condensational and coagulation growth of cloud particles, precipitation sink

The response of cloud liquid water path (LWP) and cloud fraction (CF) to altered cloud droplet number concentrations is among the most important and most uncertain adjustment mechanisms for aerosol-cloud interactions (see e.g. Maahn et al., 2021). These responses depend on the details of the cloud microphysics, particularly condensation and coagulation (and coalescence) of the cloud droplets, which are typically heavily parameterized in global models but also subject to large uncertainties in the process level. FORCeS uses in particular LES modeling, field observations and satellite data to understand these processes and improve their descriptions in ESMs (see e.g. Kim et al., 2020; Spill et al., 2021; Gryspeerd et al., 2021; Zhang et al., 2021). Many of the first published studies have dealt with improving the methodologies used in using and interpreting satellite data (alone or in combination with other data sets). Gryspeerd et al., 2021 used reanalysis wind fields and ship emission information matched to observations of ship tracks to measure the timescales of cloud responses to aerosol in instantaneous (or “snapshot”) images taken by polar-orbiting satellites. Besides highlighting the importance of the meteorological environment, this work demonstrated the importance of accounting for the time evolution of the cloud response and the aerosol source, especially in the case of an isolated aerosol source where there is no replenishment of the particle loadings. Kim et al. (2020), on the other hand, developed a novel machine-learning-based retrieval technique for obtaining LWP from satellite observations.

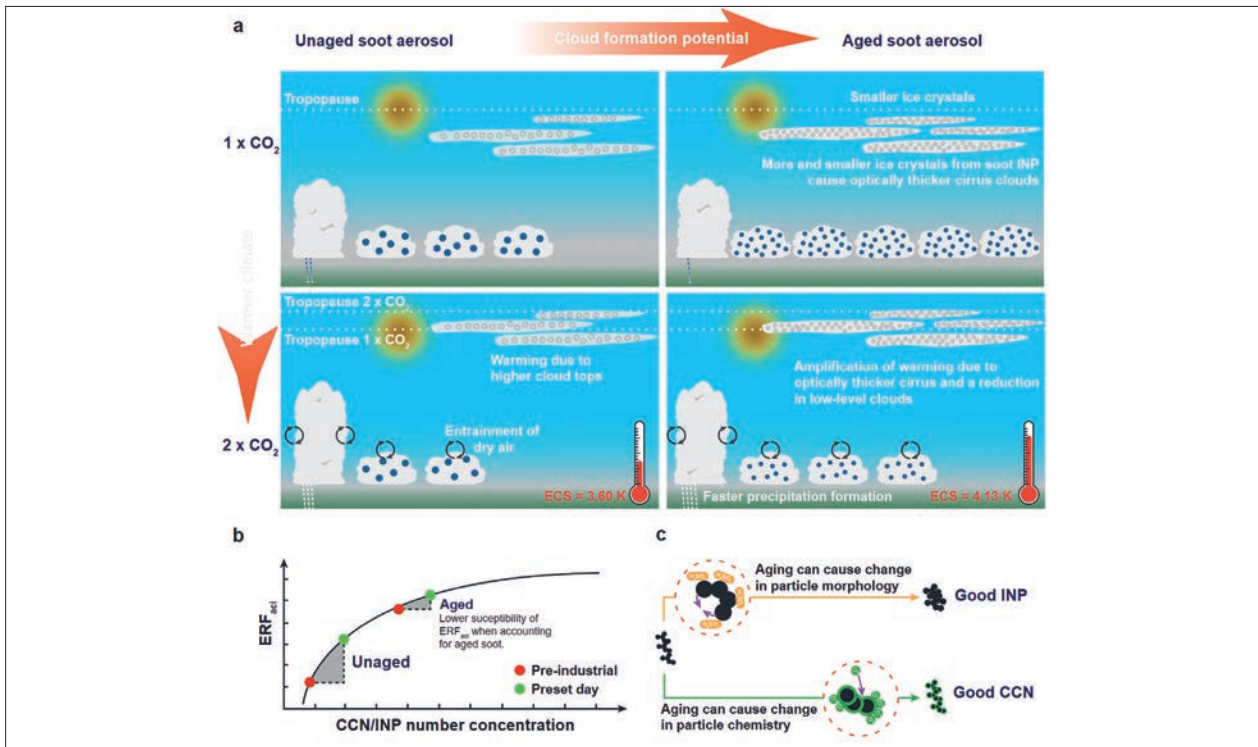


Figure 14. a) Cloud microphysical properties for the simulation of unaged (left) and aged (right) soot particles, respectively, for $1 \times \text{CO}_2$ (top) and $2 \times \text{CO}_2$ (bottom) concentrations. **b)** Qualitative change in ERF_{net} due to anthropogenic aerosol perturbations with and without accounting for the CCN and INP activities of aged soot particles. **c)** Soot particle aging types considered in the parameterizations. Figure from Lohmann et al., 2020. Reproduced under Creative Commons 4.0 (CC 4.0) license.

Task 2.3: Ice nucleation, secondary ice and freezing

Ice nucleation, secondary ice and freezing have been some of the key topics explored within the NASCENT campaign in the Arctic (see Pasquier et al., 2021; Schmale et al., 2020), and the analysis of the observations is ongoing. The new results from the dedicated campaigns related to FORCeS will be connected to previous observations on ice nuclei measurements in Ny Ålesund that are available since 2018, including the results from sample offline analysis (PM1 and PM10 using the membrane filter technique) discussed in Rinaldi et al. (2021). Rinaldi et al. 2021 discuss implications for ice nuclei origin from local terrestrial (dust), marine and distant (Arctic haze pollution), also noting that the majority of the ice-nucleating particles (INP) on the site were fine particles, although the coarse INP contribution increased somewhat during the summer (Fig. 15).

Sotiropoulou et al., 2021a discussed the importance of secondary ice processes as a source of ice crystals in Antarctic clouds and highlighted the need to understand this process better. Sotiropoulou et al. (2021b) used LES simulations to investigate the potential of ice multiplication from breakup upon ice-ice collisions could account for the observed cloud ice in a stratocumulus cloud observed during the Arctic Summer Cloud Ocean Study (ASCOS) campaign. The results from this work suggested that the overall efficiency of this process in these conditions is weak; increases in fragment generation were compensated for by subsequent enhancement of precipitation and sub-cloud sublimation. The largest uncertainty in the simulations stems from the correction factor for ice enhancement due to sublimation included in the breakup parameterization. These results indicate that the lack of a detailed treatment of ice habit and rimed fraction in most bulk microphysics schemes is perhaps not detrimental for the description of the collisional breakup process in the examined conditions as long as cloud-ice-to-snow autoconversion is considered. On top of these Arctic-focused studies, Proske et al. (2021) have demonstrated a mechanism of natural cloud seeding of lower-level clouds by ice clouds over Switzerland, while Villanueva et al. (2021) have taken a global view and used satellite observations of the hemispheric and seasonal contrast in cloud top phase to assess the dust-driven droplet freezing in the ECHAM-HAM model. Quaas et al. (2021) investigated the impact of the COVID-19 recovery plans for aviation-induced cirrus clouds.

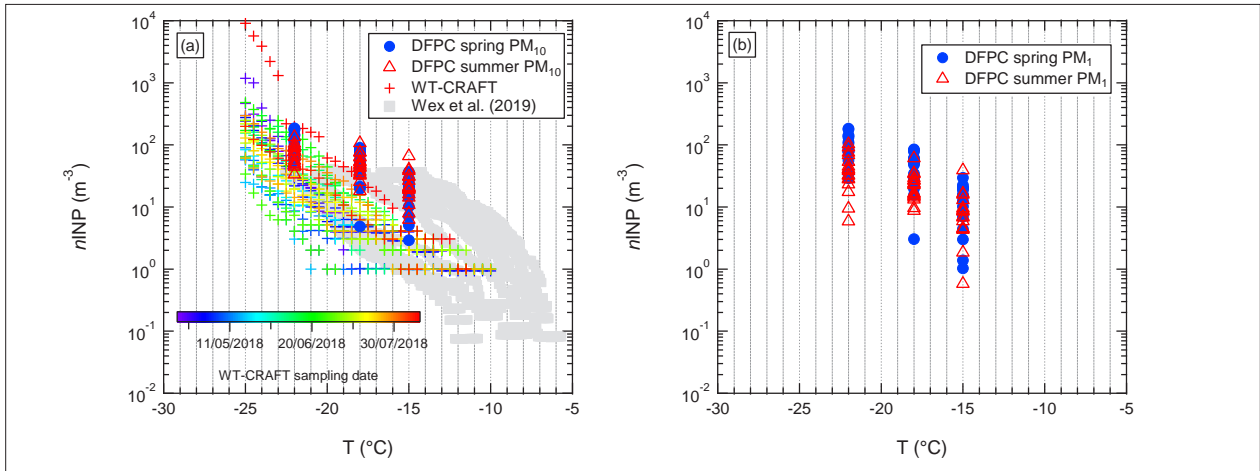


Figure 15. Ambient n_{INP} as a function of the activation T assessed for samples from Gruvbadet (GVB) during 2018 by Dynamic Filter Processing Chamber (DFPC) and West Texas Cryogenic Refrigerator Applied to Freezing Tests (WT-CRAFT). DFPC data are divided into spring (blue) and summer (red) samples, while WT-CRAFT data are color-coded according to the sampling date. (a) PM_{10} (DFPC) and TSP (WT-CRAFT) data. (b) PM_1 data (available only for DFPC). For comparison purposes, the data from Wex et al. (2019b), which refer to PM_{10} samples, are also reported in panel (a) (Wex et al. (2019a)). Adopted from Rinaldi et al., (2021). Reproduced under Creative Commons 4.0 (CC 4.0) license.

To investigate the fundamental ice properties on the molecular scale, molecular dynamics and kinetic model studies of ice crystal growth, interactions between ice and organic molecules, and the dynamics of the Wegener-Bergerron-Findeisen (WBF) process have been conducted (Schlesinger et al. 2020). This study targeted particularly the accommodation of water molecules arriving from the gas phase to the crystal structure, and concluded the order parameter (instead of energy) to be the main factor differentiating the ice surface from the bulk crystal (Fig. 16). Figure 17 illustrates the time scales of the accommodation processes related to e.g. the time scales of the relevant atmospheric processes.

Task 2.4: Entrainment and mixing as cloud sink

Much of the work conducted within Task 2.4 is directly linked to work done for Tasks 2.1 and 2.2 – since LES simulations, satellite observations, and large-scale model evaluation typically give an integrated view on the cloud responses to aerosol perturbations. Entrainment and mixing are among the key processes playing into explaining cloud responses to various types of aerosol perturbations (Maahn et al., 2020; Gryspeerd et al., 2021; Christensen et al., 2021; Zhang et al., 2021) as well as long-term trends (Cherian and Quaas 2021).

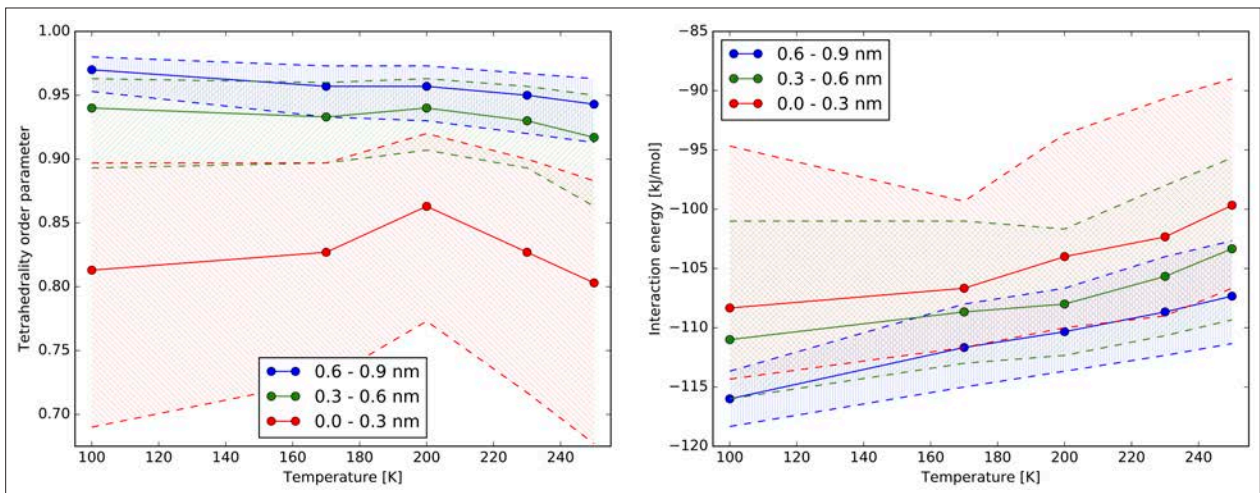


Figure 16. Medians of the distributions of tetrahedrality parameters (left) and interaction energies (right) as functions of temperature for the three topmost 3 Å layers. The hatched areas depict the width of the distributions as 25–75 quartiles. Figure from Schlesinger et al., 2020. Reproduced under Creative Commons 4.0 (CC 4.0) license.

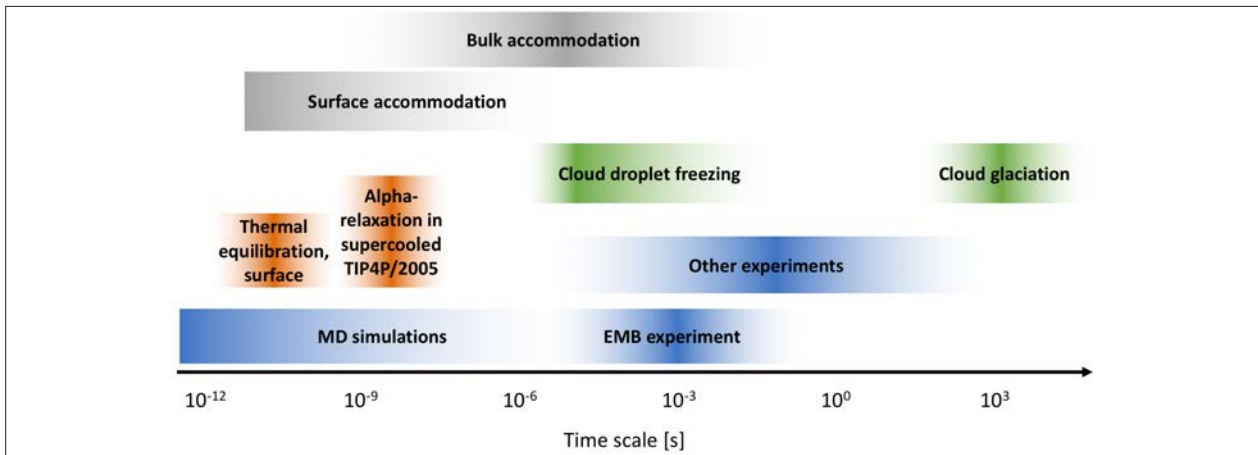


Figure 17. Schematic illustrating the time scales of different methods and phenomena of interest in the context of accommodation processes. Figure from Schlesinger et al., 2020. Reproduced under Creative Commons 4.0 (CC 4.0) license.

Task 2.5: Aerosol processing and scavenging

A key aspect related to the Puijo SMEAR IV campaign was the investigation of aerosol and vapour processing by clouds. The main measurement setup during the campaign included two sites: a ground-based site and in-cloud site allowing simultaneous investigation of the gas phase and aerosol phase constituents below the cloud and in the cloud. After the campaign, the data processing has been in an active phase. Long-term observations on cloud scavenging of absorbing aerosol components at the Puijo station were analysed (Ruuskanen et al. 2021). These observations provide an estimate on the partitioning of black carbon on different sized aerosol particles, and how efficiently those are scavenged by cloud droplets. This information is highly relevant for the evaluation of BC wet scavenging processes in large-scale atmospheric models. Aerosol wet deposition analysis based on long-term data for other aerosol components is ongoing. The results from Puijo will be contrasted and compared to the results collected during the NASCENT campaign, and to a pilot study conducted at the Åre mountain in central Sweden (Graham et al. 2020). While the scavenging of aerosol particles was clearly visible in the aerosol size distribution observations in this work, no indication of significant chemical processing in the form of e.g. aqueous-phase SOA formation was observed.

We have also investigated the processes that affect gas transport within deep convective clouds (Bardakov et al. 2021). Using LES, we have produced individual parcel trajectories within a simulated deep convective cloud. A box model has then been coupled to these trajectories to calculate e.g. gas condensation on hydrometeors, gas-phase chemical reactions, gas scavenging by hydrometeors and turbulent dilution. We find that the trace gas transport approximately follows one out of three scenarios, determined by a combination of the equilibrium vapor pressure (containing information about water-solubility and pure component saturation vapor pressure) and the enthalpy of vaporization (see Fig. 18 for the ranges of molecular properties considered by Bardakov et al., 2021). In one extreme, the trace gas will eventually be completely removed by precipitation. In the other extreme, there is almost no vapour condensation on hydrometeors and most of the gas is transported to the top of the cloud. The results from Bardakov et al. (2021) on the isoprene system show that gas uptake to anvil ice is an important parameter for regulating the intensity of the isoprene oxidation and associated low volatility organic vapor concentrations in the outflow.

5.3 Progress within WP3 “Role of aerosol and cloud changes for aerosol radiative forcing between 1950 and 2050”

FORCeS WP3 investigates the temporal development of key aerosol components, their physical characteristics, as well as cloud changes between 1950 and 2050 using different scenarios. The specific objectives of WP3 include:

- Determining transient changes in aerosols and clouds and the corresponding ERF from 1950 to present day,
- Understanding and quantifying the key uncertainties in the aerosol forcing between 1950–2050,
- Providing plausible near-future projections of ERF.

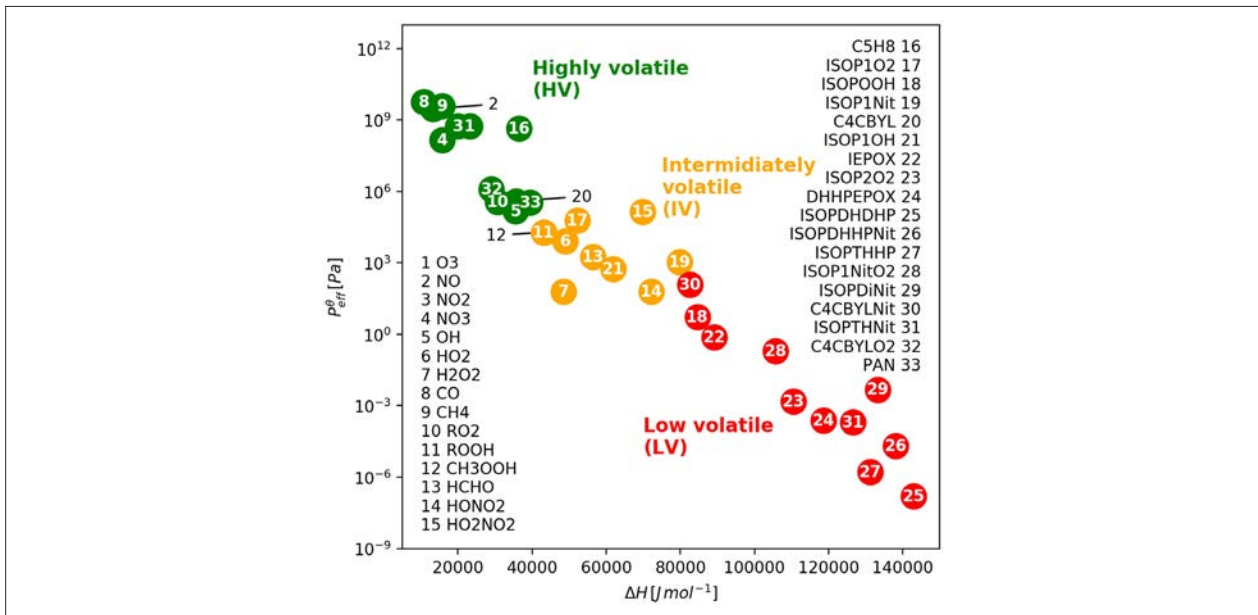


Figure 18. Volatility diagram for the compounds simulated by Bardakov et al. (2021). Reproduced under Creative Commons 4.0 (CC 4.0) license.

The scientific work in WP3 has proceeded generally as described in the DoA.

This WP undertakes to determine aerosol-related changes from 1950 to the present day through coordinated FORCeS ESM model simulations. Transient aerosol records have been produced using three FORCeS ESMs using aerosol schemes of different levels of complexity and different host climate characteristics. All three models are well documented (Seland et al. 2020; Neubauer et al. 2019; van Noije et al. 2020). Relevant model data for the period 1950–present has been assembled and published under CMIP6 ESGF nodes. The three FORCeS ESMs have been diagnosed for aerosol composition and radiative property diagnostics based on their AeroCom and CMIP6 simulations (Gliß et al. 2021). The three models, altogether provide a rather representative spread of the wider CMIP6 and AeroCom ensemble. A corresponding comprehensive large observational data set of the aerosol physical properties and composition evolution has been assembled from in-situ data, wet deposition and ice core data and satellite remote sensing since 1979. The trends in models and observations 2000-2014 have been found to be similar to the first order (Mortier et al. 2020). A comparison to incoming surface radiation shows significant and unexplained bias in Asia which may hint at emission uncertainties (Onsum Moseid et al. 2020).

Task 3.1: Determine aerosol and cloud changes 1950-present

Three types of experiments have been performed with the FORCeS ESMs which are crucial for the documentation and analysis of the historical aerosol forcing record:

- AeroCom phase III *control* and *historical* atmospheric simulations nudged to reanalysed meteorology. These simulations have been conducted for the year 2010 and the period 1750–2014 using the same emissions as CMIP6. Note, that the three models cover the 1750–2014 period in differing levels of detail.
- CMIP6 coupled ESM *historical* simulations and perturbations of that using pre-industrial aerosol emissions (*hist-piAer*). These simulations are part of the DECK (Eyring et al. 2016) and AerChemMIP model intercomparisons (Collins et al. 2017). These simulations are complete for the three FORCeS ESMs.
- CMIP6 AGCM simulations with sea surface temperature fields derived from the historical simulation (*histSST*) and the corresponding perturbed simulation with pre-industrial aerosol (*histSST-piAer*) are the basis for the calculation of the evolution of the aerosol ERF. These simulations are available from NorESM and MPI-ESM, and are in the process of being comprised for EC-EARTH as well. The analysis of these simulations will be done once all data are available.

Extensive analysis and discussion on the various aspects of aerosol loadings in recent history based on the available simulations has been published within Mortier et al. (2020), Allen et al. (2020), Turnock et al. (2020), Lee et al. (2021), Gliß et al. (2021), Su et al. (2021) and Onsum Moseid et al. (2021); only very brief highlights will be provided here.

Figure 19 shows the regional AOD trends for different aerosol components from the 11 different AeroCom and CMIP6 models compared to observational data as analysed for the period of 2000–2014 by Mortier et al., 2020. The results reveal that the observations exhibit mostly negative trends of the extensive parameters in the different regions of the world. Significant decreases are found in Europe, North America, South America, North Africa and Asia. In Asia, the aerosol extinction (AE) increases in time and is consistent with increases in AOD_f (f referring to fine) and SO₄, which reflects a regional increase in the anthropogenic aerosols in that region in the overall study period from 2000 to 2014. The models tend to capture observed AOD, AE, SO₄ and particulate matter (PM) trends but show larger discrepancies regarding AOD_c (c referring to coarse). The rather good agreement of the trends across different aerosol parameters between models and observations, when co-locating them in time and space, implies that global model trends, including those in poorly monitored regions, are likely correct.

A comprehensive analysis and evaluation of various aspects of the aerosol life cycle, budgets and optical properties for the reference year 2010 from 14 different models participating in the AeroCom Phase III Control Experiment was conducted by Gliß et al. (2021). For instance, the analysis of aerosol budgets for sulfate, black carbon, organics, dust, sea salt and nitrate show significant differences in aerosol lifetime between the models (see Fig. 20 for an overview of the model intercomparison).



Figure 19. Regional trends in the aerosol properties computed with observations and models co-located in space and time with the observations. The error bars correspond to the uncertainty in the trend as calculated using both the uncertainty in the Theil–Sen slope and the residuals. The bold font indicates that the trends are significant at a confidence level of 95 % (p -value < 0.05). For an explanation of the parameters, see Mortier et al., 2020. Reproduced under Creative Commons 4.0 (CC 4.0) license.

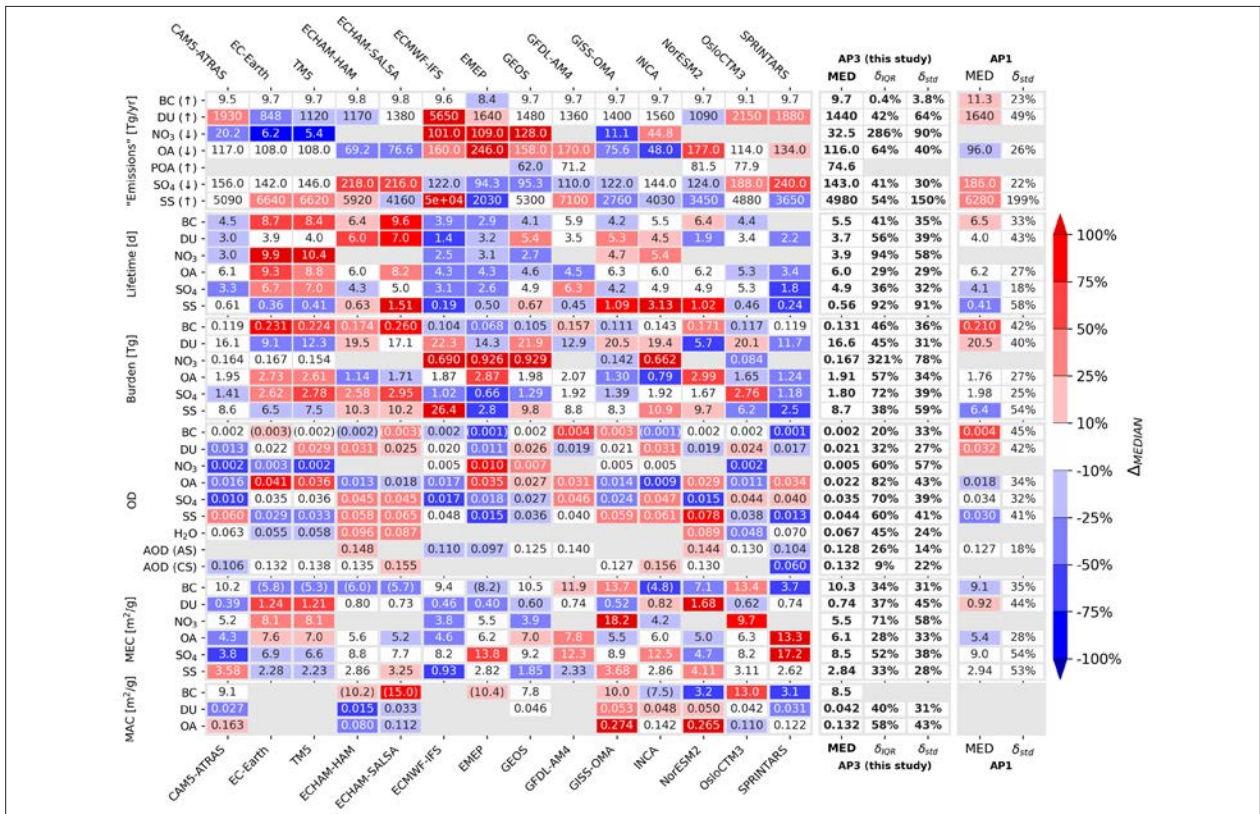


Figure 20. Global annual averages for each aerosol species, grouped by aerosol emissions, lifetimes, burdens, optical depths (ODs), mass extinction coefficients (MECs), and mass absorption coefficients (MACs), for models participating in the AP3-CTRL experiment, in the year 2010. Also shown in the OD section are total AOD for all-sky (AOD (AS)) and clear-sky (AOD (CS)) conditions as well as AOD due to water (H₂O). The following columns show the median from all model values (MED) and associated diversities as interquartile range and standard deviation (δ_{IQR} , δ_{std}). Colours illustrate the bias of individual model and AP1 (AeroCom Phase I) median values with respect to the AP3 (AeroCom Phase III) median. Units of emissions and burdens are full molecular weight (for OA and POA, the total organic weight is used). Note that the “emissions” of SO₄, NO₃, and OA are really secondary chemical formation in the atmosphere plus primary particle emissions. They are computed using total deposition as a proxy (indicated with ↓). For BC↑, DU↑, POA↑, and SS↑ the provided emission data were used. For OsloCTM3 an additional OD of 0.0086 due to biomass burning was reported and is not included here. Further details are available in Gliß et al. (2021). Reproduced under Creative Commons 4.0 (CC 4.0) license.

Onsum Moseid et al. (2021) investigated global and regional aerosol radiative effects over the time period 1961–2014 by looking at surface downwelling shortwave radiation (SDSR). They used observations from ground stations as well as multiple experiments from eight ESMs participating in CMIP6. The results showed that this subset of models reproduces the observed transient SDRS well in Europe but poorly in China (see Fig. 21). The likely explanation for this was associated with missing emissions of sulfur dioxide in China, highlighting the importance of accurate emission inventories for narrowing down uncertainties in aerosol-climate interactions.

Task 3.2: Provide transient ERFari+aci records 1950-present from the available FORCeS atmospheric global models constrained by observational data

The analysis is based on the same simulations as described under Task 3.1. Comparisons made against observed radiative properties by Gliß et al. (2021), Mortier et al. (2020), Onsum Moseid et al (2020) suggest that the ERFari effect is underestimated in the FORCeS models – similarly to the majority of the other models analysed. Both optical depth and surface aerosol scattering are underestimated significantly as shown in Fig. 22 (Gliß et al. 2021). Comparison with cloud properties and thus ERFaci estimates are ongoing.

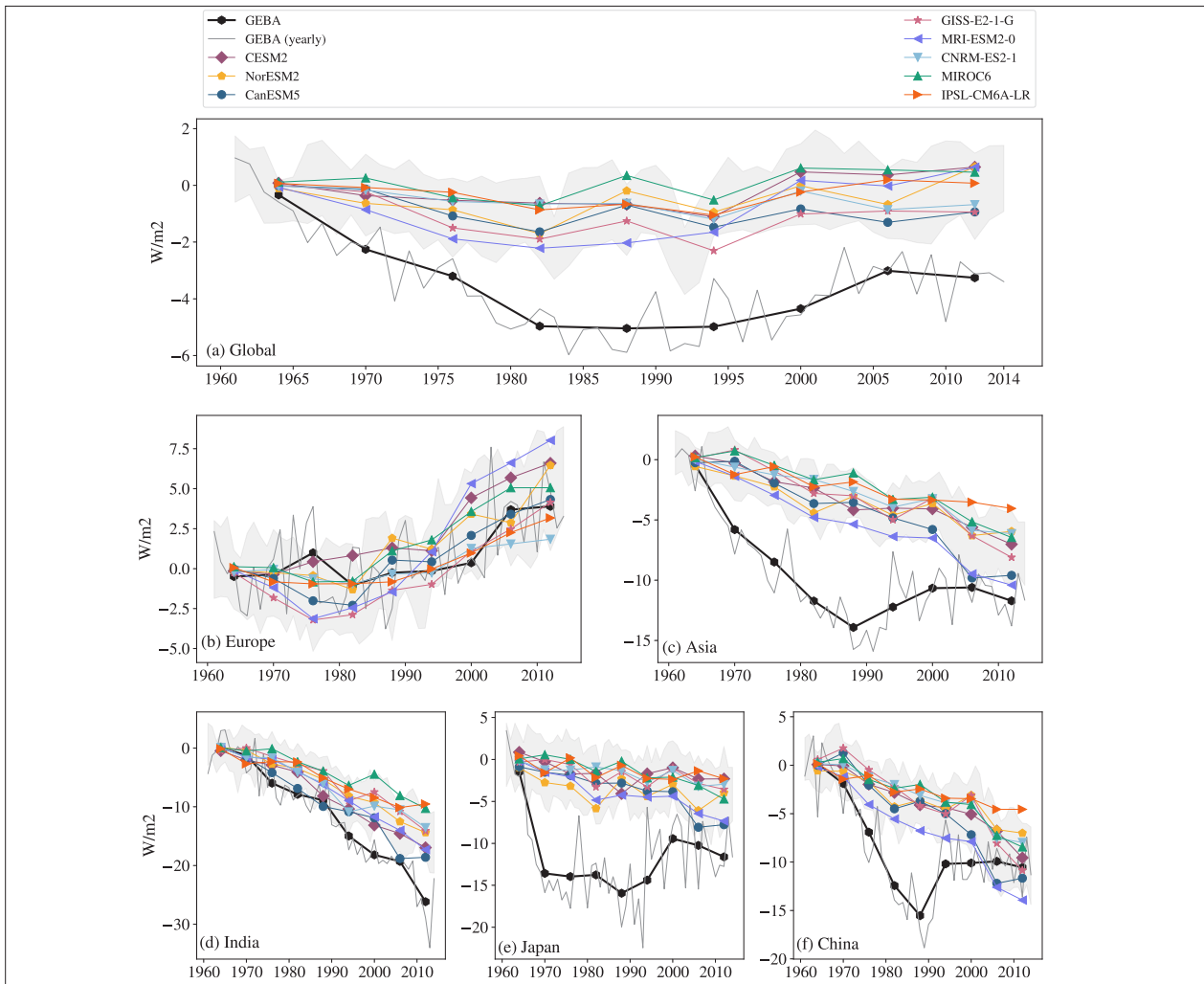


Figure 21. Six-year averages of the SDRS anomaly at the surface for GEBA and eight Earth system models. Results are co-located at (a) all GEBA stations (1487), (b) European (503), (c) Asian (311), (d) Indian (15), (e) Japanese (100), and (f) Chinese (119) stations. Numbers in parentheses are the number of ground stations in the respective region. The entire 54-year period has been divided into intervals of 6 years and then averaged together to make nine data points as shown by the markers. The grey shading represents 1 standard deviation from the yearly total ensemble mean. Reproduced under Creative Commons 4.0 (CC 4.0) license.

Task 3.3: Determine the main contributions to model uncertainty to the simulated transient ERF (1950-2050) using perturbed physics ensembles and emulators

The work towards this Task is ongoing using an open-source software for the emulator setup (Watson-Parris et al., 2021) but there are no publications directly from FORCes on this work yet.

Task 3.4: Provide several likely near future (until 2050) aerosol composition and ERF_{ari+aci} trends

Although the work within this Task was scheduled to start only during the second half of FORCes, the piloting work within e.g. Allen et al., 2020; Turnock et al., 2020 and Fiedler et al., 2021 already provide some first insights into the future trends.

5.4 Progress within WP4 “Novel constraints on aerosol radiative effects”

Four of the WP4 tasks are targeted towards developing and applying novel ways of constraining models: process scale-chains, natural analogues, long-term transient constraints and perturbed parameter ensembles (see Tasks 4.2–4.5 below). Another role of WP4 is to act as a “data-hub” for the project (see Task 4.1 below). Overall, the work within WP4 has progressed according to the plan laid out in the DoA.

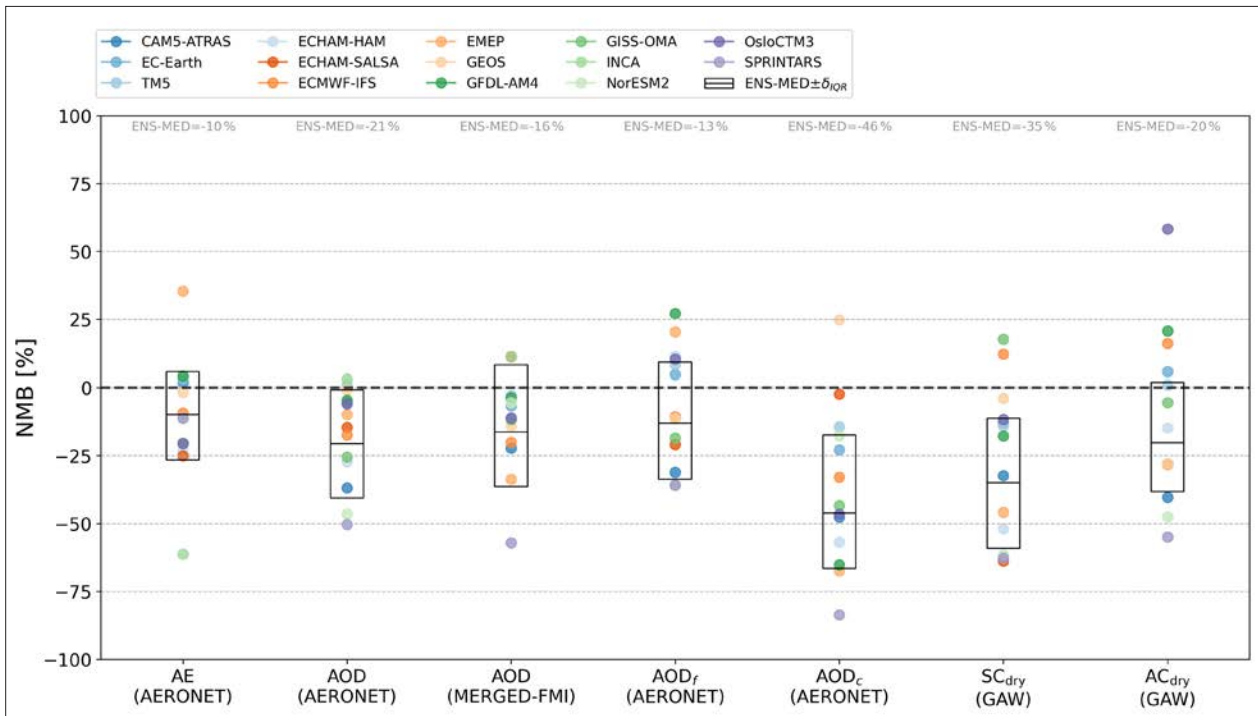


Figure 22. Summary of results from comparison of models with ground-based observation networks and MERGED-FMI satellite AOD data set. The y axis indicates the retrieved biases (NMBs) for individual models (indicated as circles). The black boxes indicate results from the ensemble median (ENS-MED), together with the associated spread (δ_{IQR}). AOD: Aerosol optical depth, AE Angström exponent, SC: surface scattering coefficient, AC: surface absorption coefficient (figure from Gliß et al. 2021). Reproduced under Creative Commons 4.0 (CC 4.0) license.

Task 4.1: Synthesis of in-situ and remote sensing observations

WP4 has conducted scoping work of the data used and produced within FORCeS, which includes data from laboratory studies, field observations, remote sensing and various kinds of model output datasets (see for e.g. Väisänen et al., 2020; Kim et al., 2020; Paglione et al., 2021; Pasquier et al., 2021; Wu et al., 2021; Gryspeerdt et al., 2021; Herbert et al., 2021; Gliß et al. 2021). Most of the work during the first two years has been directed towards facilitating the internal communication and data exchange within the project, but as new original results are being published as a result of FORCeS, more effort will be directed also towards dissemination of the results to outside of the consortium as well, in line with the principles outlined within the FORCeS Data Management Plan (DMP).

Task 4.2: Observational constraints along the scale chain

The compilation and collection of data sets used and produced by FORCeS allows for the design of novel observational constraints that propagate over different scales – from process-level understanding to regional and global scale impacts. In addition, significant progress has already been made on the development of metrics and methodologies for observational constraints along the scale chain, including, but not limited to novel approaches to understand aerosol-cloud interactions and feedbacks in a regime-based context. In the following, we will give some highlights on the scientific work conducted so far within FORCeS that includes an element of moving over scale boundaries.

A recent study by Yli-Juuti et al. (2021) combined long-term in-situ observations of meteorological parameters, aerosol size distribution and chemical composition to collated remote sensing observations on cloud and aerosol properties, in order to study and quantify the feedback between temperature, aerosol loadings and cloud properties in the boreal region (see Fig. 23). Summer time OA loadings showed a clear increase with temperature (see also e.g. Heikkinen et al., 2021), with a simultaneous increase in CCN concentration in a boreal forest environment. Remote sensing observations revealed a change in cloud properties with an increase in cloud

reflectivity in concert with increasing organic aerosol loadings in the area (see Fig. 24). The results provide direct observational evidence on the significance of this negative climate feedback mechanism.

A new framework for the definition of dynamical regimes for cloud forcing and feedback studies has been developed (Douglas and Stier, 2021). This method is based on the analysis of global satellite datasets, objectively clustering cloud (parameter) controlling environmental factors derived from gradient boost regression and neural network machine learning models to determine the dominant combination of cloud controlling factors for each region. This approach provides a new way to control for confounding factors in the causal attribution of aerosol climate effects and feedback studies as well as a new way to evaluate the representation of clouds in ESMs. A complementary approach, attributing model-simulated ERF_{aci} to objectively clustered cloud regimes (based on k-means clustering in cloud-top-height / cloud optical depth space) has been developed and applied to the model UKESM (Langton et al., 2021, see Fig. 25).

A review of our current understanding of observational constraints on the Twomey effect from satellite observations has also been conducted (Quaas et al. 2020, see also Sect. 5.2), highlighting underlying uncertainties in the quantification of (i) the cloud-active aerosol – the CCN concentrations at or above cloud base, (ii) cloud droplet number concentrations, (iii) the statistical approach for inferring the sensitivity of N_d to aerosol particles from the satellite data and (iv) uncertainty in the anthropogenic perturbation to CCN concentrations, which is not easily accessible from observational data. Such observational constraints, as illustrated in Fig. 26, can be used to constrain models across the scale chain (see also Section 5.2).

Task 4.3: Natural and anthropogenic analogues of aerosol-cloud interactions

This task strives towards establishing a set of observations representative of different natural and anthropogenic analogues from satellite and in-situ data. The work within this Task has only been ongoing for a year (since M12 of the project), but some scientific progress has already been made and results published. Some highlights from the work done so far are presented below.

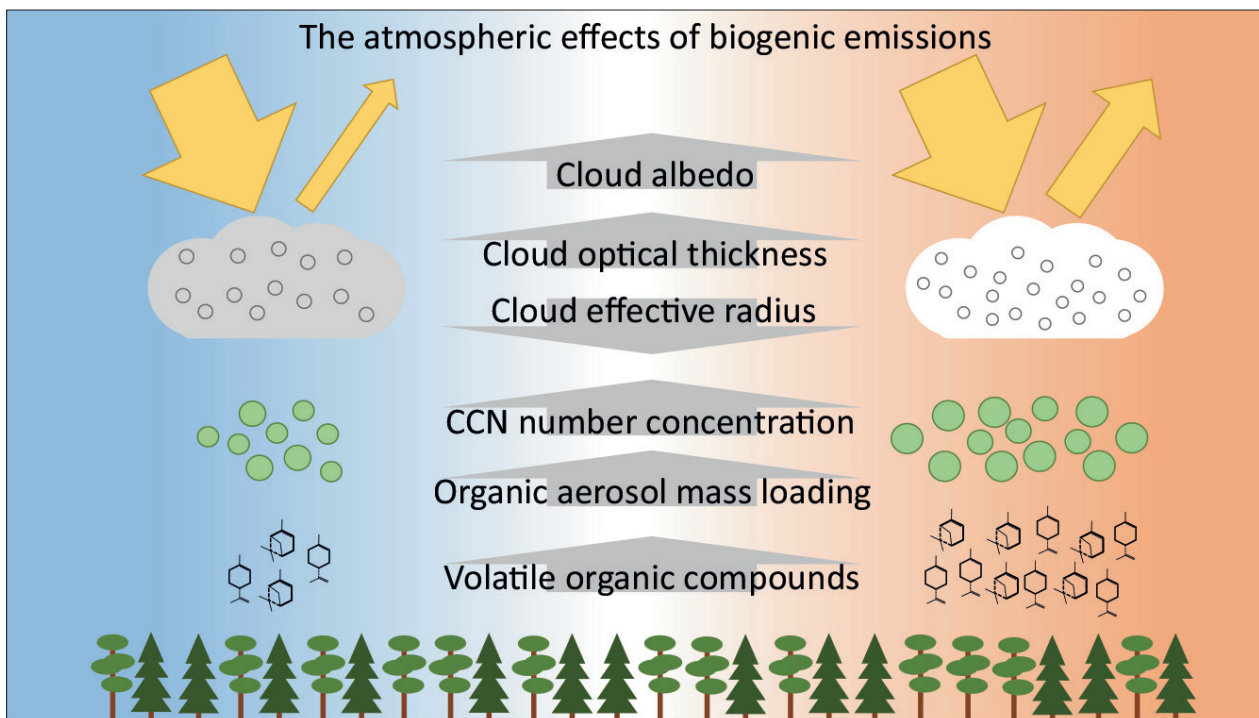


Figure 23. In warmer conditions (on right), volatile organic compound (VOC) emissions from vegetation are higher compared to colder condition (on left). Consequently, more VOC are available for oxidation and forming BSOA. This leads to higher organic aerosol mass loading and higher cloud condensation nuclei (CCN) number concentration. These in turn lead to higher number but smaller size of the cloud droplets, increased cloud optical thickness, and consequently to stronger aerosol indirect effect on climate (adopted from Yli-Juuti et al., 2021). Reproduced under Creative Commons 4.0 (CC 4.0) license.

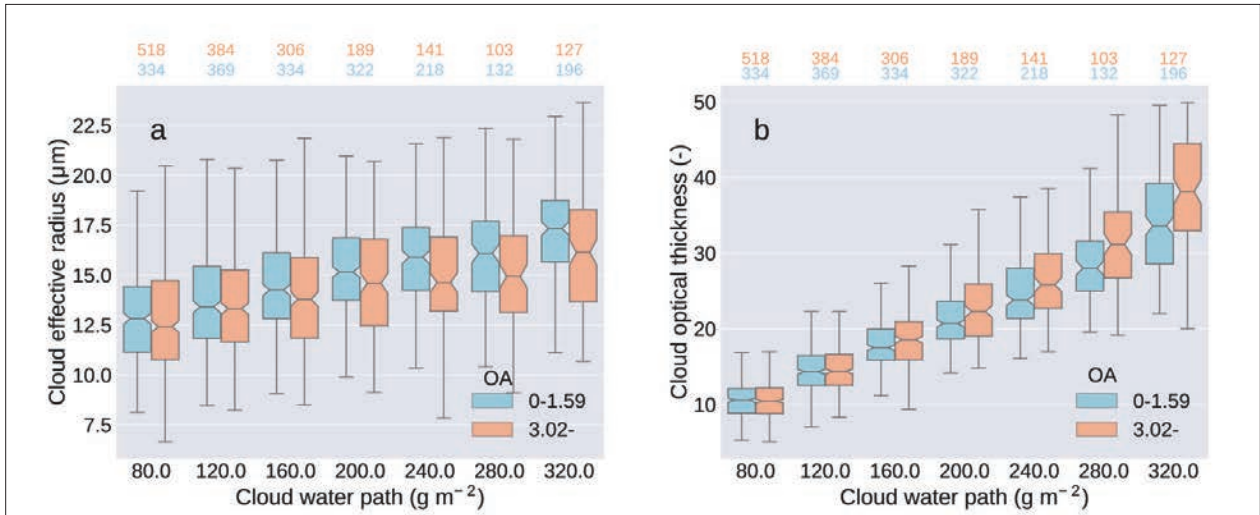


Figure 24. **a** Cloud effective radius and **b** cloud optical thickness divided based on the level of cloud water path. Data are divided into low (<33rd percentile ($1.59 \mu\text{g m}^{-3}$), blue) and high (>66th percentile ($3.02 \mu\text{g m}^{-3}$), red) organic aerosol (OA) mass loadings. The box shows the quartiles of the dataset while the whiskers show the rest of the distribution, except for points that are determined to be “outliers” using a method that is a function of the inter-quartile range. The notch in the box displays the confidence interval around the median. The blue and red numbers above each figure indicate the number of data points in each box (adopted from Yli-Juuti et al., 2021). Reproduced under Creative Commons 4.0 (CC 4.0) license.

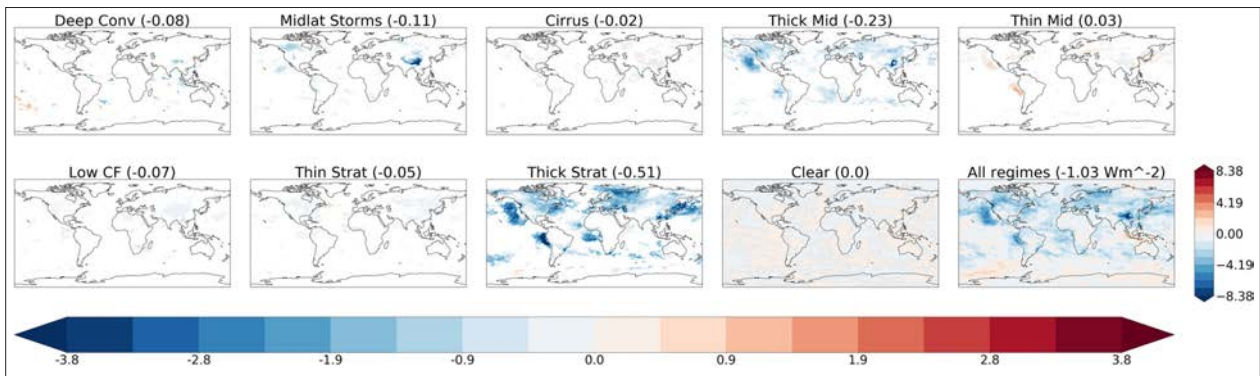


Figure 25. Decomposition of UKESM simulated effective radiative forcing from aerosol-cloud interactions of all regimes (lower right) into objectively clustered cloud regimes (Langton et al., 2021). Reproduced under Creative Commons 4.0 (CC 4.0) license.

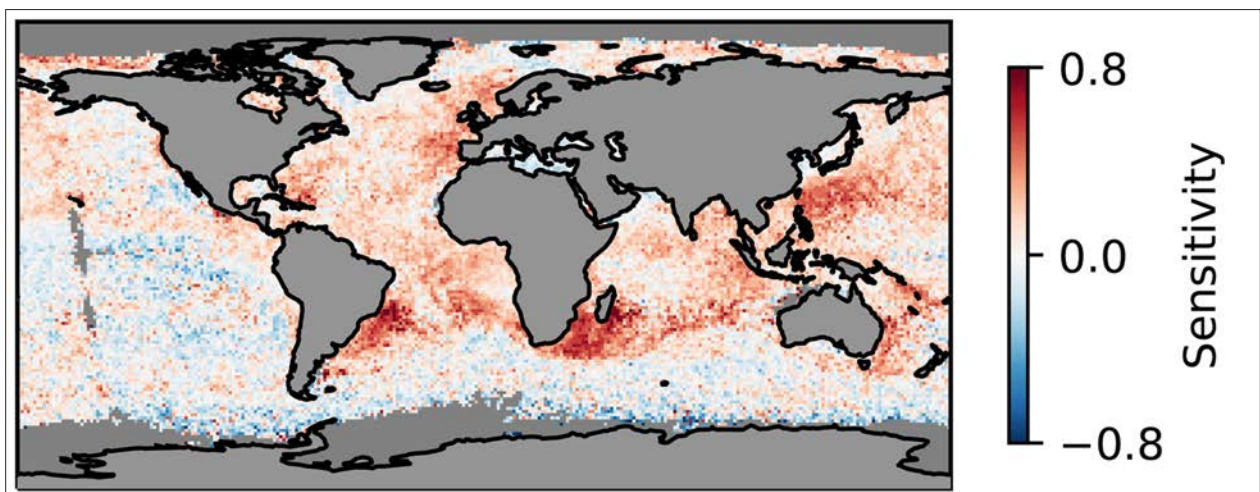


Figure 26. Droplet number sensitivity to aerosol index as derived from the MODIS satellite sensor for daily temporal variability (adopted from Quaas et al., 2020). Reproduced under Creative Commons 4.0 (CC 4.0) license.

The work by Maahn et al. (2021), Gryspeerdt et al. (2021) and Herbert et al. (2021) focused on analysing cloud responses to well-constrained aerosol perturbations in different types of environments: industrial emissions to the clean Arctic atmosphere, emissions from ships to the marine boundary layer and biomass burning plume in the Amazon (see also Sect. 5.2). As an example, Maahn et al., (2021) used anthropogenic emissions at the North Slope of Alaska as a natural laboratory to study relationships between aerosols and Arctic liquid-containing clouds. Averaging 14 years of MODIS satellite observations, a reduction in temporally averaged cloud effective radius (r_e) of up to 1.0 μm related to localized pollution was observed, with potentially significant implications for radiative forcing. Due to the frequent occurrence of liquid-containing clouds, this implies that enhanced local emissions in Arctic regions can impact climate processes.

Task 4.4: Constraints for the transient aerosol forcing record

The work within this Task has just started (M24 of the project) and hence there are no published results to report yet.

Task 4.5: Bottom-up observational constraint of modelled decadal changes in aerosols and radiative forcing

The work within this Task has just started (M24 of the project) and hence there are no published results to report yet.

Task 4.6: Community evaluation tools for aerosols and clouds in support of IPCC

The work within this Task has just started (M24 of the project) and hence there are no published results to report yet.

5.5 Progress within WP5 “Climate response and feedbacks within ESMs”

Overall, the work within WP5 has progressed according to the plan, and WP5 collaborates closely with WPs 3 and 6 (see Sects. 5.3 and 5.6). The specific objectives of WP5 are to analyze simulated climate response, feedbacks and sensitivities to aerosol and cloud forcing in ESMs, quantify the simulated responses to specific key processes and their effects in regional focus areas, and improve the simulation of processes relevant for regional and global sensitivities. During the first two years, the work within WP5 has focused on analyzing existing simulations in the CMIP6 archive (and other suitable archives, e.g. CMIP5, AeroCom) to assess the climate response, feedback and sensitivities to aerosol and cloud forcing. Some of the studies performed in WP5 have looked at the global response while others have had a more regional focus. The implementation of new and improved parameterizations into the FORCES ESMs has started in M15 and is guided by the analysis done in T5.1 together with input from other WPs.

Task 5.1: Identification of relevant processes for response and feedbacks to aerosol and cloud forcing

The goal of this task is to analyse and better understand the role aerosols play in climate model simulations, in particular the CMIP6 experiments and with a special focus on the three FORCES ESMs. There has been substantial progress along these lines in the form of both multimodel studies (e.g. Wyser et al., 2020; Gliß et al., 2020; Sand et al., 2020; Turnock et al., 2020; Mortier et al., 2020; Cherian and Quaas, 2021; Su et al., 2021; Dagan et al., 2021) as well as detailed studies focusing on specific models (e.g. Frey et al., 2021; Krishnan et al., 2020; Spill et al., 2021; Langton et al., 2020; Lohmann et al., 2020; Zhang et al., 2021; Li et al., 2021; Villanueva et al., 2021; Fiedler et al., 2021) – the results from many of which have already been discussed above. In the following, some further highlights from this work conducted so far are presented.

Su et al. (2021) analysed biases in aerosol optical depths (AOD) and land surface albedos in the AeroCom models, which manifest themselves in the top-of-atmosphere (TOA) clear-sky reflected shortwave (SW) fluxes. Biases in the SW fluxes from AeroCom models were quantitatively related to biases in AOD and land surface albedo by using their radiative kernels. It was found that over ocean, AOD contributes to about 25% of the 60S–60N mean SW flux bias for the multi-model mean (MMM) result. Over land, AOD and land surface albedo contributed to about 40% and 30%, respectively, of the 60S–60N mean SW flux bias for the MMM result. Su et al. (2021) also

compared the AOD trend from three models with the observation-based counterpart. These models reproduce all notable trends in AOD except the decreasing trend over eastern China and the adjacent oceanic regions due to limitations in the emission data set (see also Onsum Moseid et al., 2021 and Section 5.3).

Turnock et al. (2020) analysed the key air pollutants, specifically O₃ and PM_{2.5} predicted for years 2000–2014 and projected for the near-future of years 2015–2100 by 11 models participating in CMIP6. An evaluation of these models against surface observations of O₃ and PM_{2.5} reveals that the CMIP6 models consistently overestimate observed surface O₃ concentrations across most regions and in most seasons by up to 16 ppb, with a large diversity in simulated values over Northern Hemisphere continental regions. Conversely, observed surface PM_{2.5} concentrations are consistently underestimated in CMIP6 models by up to 10 $\mu\text{g m}^{-3}$, particularly for the Northern Hemisphere winter months, with the largest model diversity near natural emission source regions (see Fig. 27). The biases in CMIP6 models when compared to observations of O₃ and PM_{2.5} are similar to those found in previous studies. The projection of regional air pollutant concentrations from the latest climate and ESMs used within CMIP6 shows that the particular future trajectory of climate and air quality mitigation measures could have important consequences for regional air quality, human health and near-term climate (see also Allen et al., 2020 for a detailed discussion). Differences between individual models emphasize the importance of understanding how future Earth system feedbacks influence natural emission sources, e.g. response of biogenic emissions under climate change.

Wyser et al., (2020) investigated the reasons behind warmer climate projections for the 21st century in CMIP6 than in CMIP5 despite nominally identical instantaneous radiative forcing. The stronger warming in the CMIP6 projections has typically been attributed to the higher climate sensitivity of the new generation of climate models. However, Wyser et al. (2020) demonstrate that changes in the forcing datasets also can play an important role, in particular the prescribed concentrations of greenhouse gases (GHG) that are used to force the models. In the EC-Earth3-Veg model the effective radiative forcing (ERF) was reduced by 1.4 W m^{-2} when the GHG concentrations from SSP5-8.5 (used in CMIP6) are replaced by the GHG concentrations from RCP8.5 (used in CMIP5), and similar yet smaller reductions are seen for the SSP2-4.5/RCP4.5 and SSP1-2.6/RCP2.6 scenario

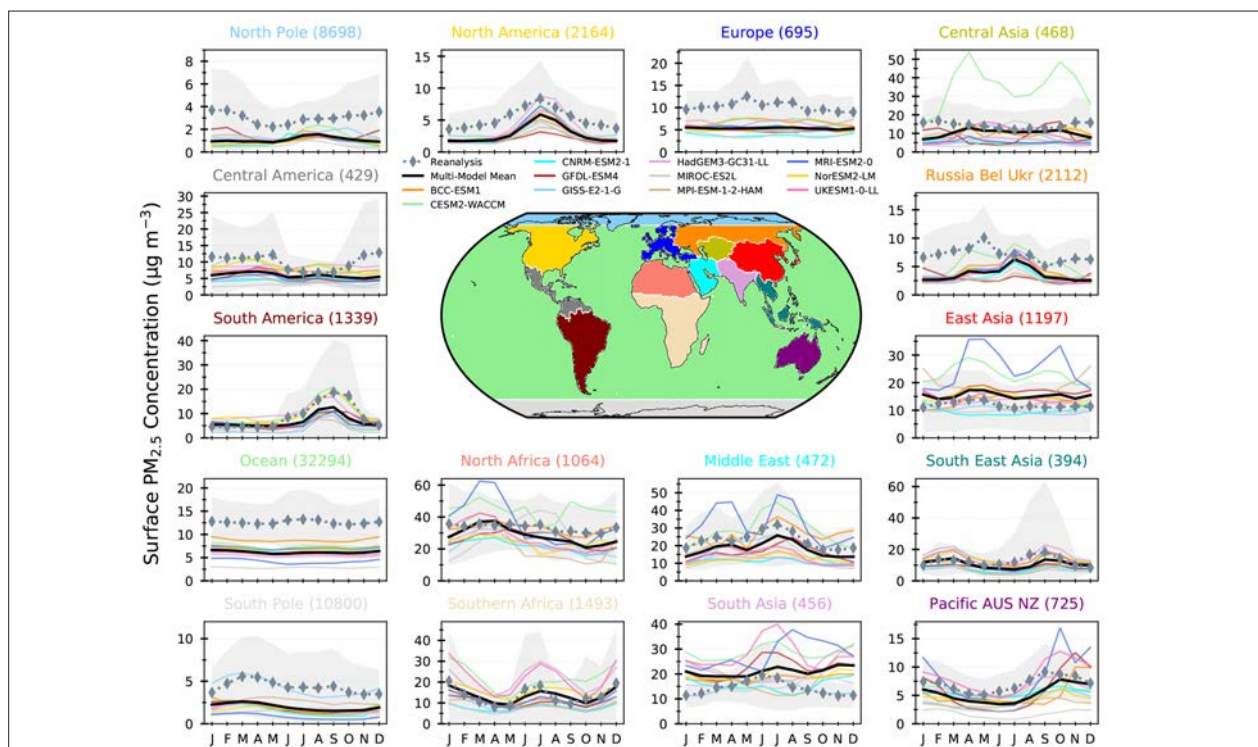


Figure 27. Individual and multi-model (11 CMIP6 models) monthly mean surface PM_{2.5} concentrations across different world regions compared with the regional monthly values from the PM_{2.5} MERRA-2 reanalysis within the region for the period 2005–2014. The number of reanalysis points within the region is shown in parentheses. The shading shows variability in the values of the MERRA-2 reanalysis products across the region. Adopted from Turnock et al. (2020). Reproduced under Creative Commons 4.0 (CC 4.0) license.

pairs. Wyser et al. (2020) also tested whether the additional forcing caused by the changes in GHG concentrations from CMIP5 to CMIP6 is possibly compensated by other changes in the SSP forcing datasets, in particular a stronger cooling from CMIP6 aerosols. There was, however, only a minor impact on the ERF in EC-Earth3-Veg.

Previous work using NorESM1-M has shown that decreases in regional SO₂ emissions lead to three key responses – an enhanced temperature response in the Arctic, a weakening of the Atlantic Meridional overturning circulation (AMOC), and anomalous poleward heat transport from the sub-polar North Atlantic into the Arctic. To better understand the enhanced temperature response, we have analyzed simulations using NorESM1-M in a slab-ocean mode (Krishnan et al., 2020). These simulations show that the atmosphere plays the primary role in driving Arctic warming in response to European aerosol reductions (see Fig. 28). A key mediator of the temperature response is a change in sea-ice extent, through modifications of turbulent flux exchanges and surface temperature. A good representation of Arctic sea ice is therefore vital for confident projections of future Arctic climate change. Further, the key to understanding this Arctic response is to constrain the specific atmospheric processes and feedbacks that drive the initial sea-ice melt.

Dagan et al. (2021), on the other hand, studied the impact of aerosol forcing on the North Atlantic Warming Hole (NAWH, i.e. the reduced warming, or even cooling, of the North Atlantic during an anthropogenic-driven global warming). A NAWH is predicted by climate models during the 21st century, and its pattern is already emerging in observations. Using output from CMIP6 simulations, Dagan et al. (2021) show that anthropogenic aerosol forcing opposes the formation of the NAWH (by leading to a local warming) and delays its emergence by about 30 years. In agreement with previous studies, we also demonstrate that the relative warming of the North Atlantic under aerosol forcing is due to changes in ocean heat fluxes, rather than air-sea fluxes. These results suggest that the predicted reduction in aerosol forcing during the 21st century may accelerate the formation of the NAWH.

Task 5.2: Implementation of revised parameterizations into ESMs

The work within this Task has started less than a year ago (M15 of the project) and hence there are no published results to report yet, but the implementation work is ongoing based on the output from WPs 1, 2 and 4.

Task 5.3: Effect of updated or simplified aerosol/cloud processes in ESMs

The work within this Task has not started (starts M32 of the project) and hence there are no published results to report yet.

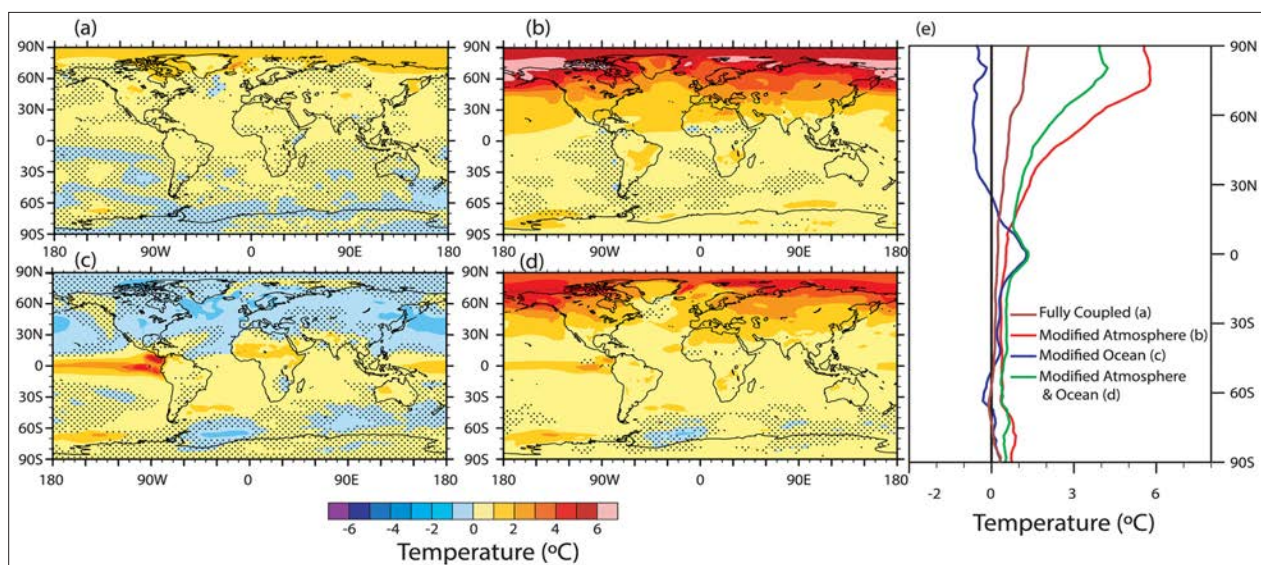


Figure 28. Spatial changes in surface temperature for (a) fully coupled, (b) modified atmosphere, (c) modified ocean, (d) modified atmosphere-ocean, and (e) zonal differences in surface temperature. Nonstippled regions are significant. Nonstippling indicates statistical significance at 95% for annual mean changes between the perturbed and the control simulations using a Student's t test. Adopted from Krishnan et al., 2020. Reproduced under Creative Commons 4.0 (CC 4.0) license.

5.6 Progress within WP6 “Constraining climate sensitivity and near-term climate response”

WP6 identifies and evaluates observable quantities that govern the transient climate response (TCR), which is the standard measure of transient climate sensitivity (TCS) in ESMs. WP6 also combines this work with statistical and simple/idealized modelling to arrive at a new central estimate and narrower uncertainty range for TCR/TCS, as well as a re-evaluation of the emission reductions needed to meet the PA. Another important task of WP6 is to use existing and develop new emergent constraints to evaluate the FORCES models.

During the first reporting period, WP6 has analyzed TCR in CMIP6 models, with particular focus on the three FORCES ESMs and their performance with respect to existing emergent constraints (D6.1). We have also started the work of developing new emergent constraints using e.g. network analysis. The work is progressing according to plan and two of the four tasks within WP6 will not start until the next reporting period.

Task 6.1: Evaluate FORCES ESMs at the beginning of the project (transient climate response and emergent constraints)

This task has been completed according to schedule, and a deliverable in the form of a report on the transient climate response (TCR) of FORCES ESMs as well as their performance with respect to established emergent constraints has been finalized and shared with the consortium (see also Meehl et al., 2020; Schlund et al., 2020; Van Noije et al., 2021).

Of relevance for this task is also recent work following up on studies using previous generation models (CMIP5, as in Grose et al. (2018)) by investigating the relationship between different measures of climate sensitivity, primarily Equilibrium Climate Sensitivity (ECS) and TCR, in CMIP6 models, and their respective “predictive power” of future temperature projection. As in CMIP5, the sensitivity measures are correlated, and they correlate with the projected temperature anomaly, but for CMIP6 models the transient measure TCR is a better predictor of the model projected temperature change from the pre-industrial state, not only on decadal timescale but throughout much of the 21st century. For strong mitigation scenarios, the difference persists until the end of the century. Regional analysis shows a superior predictive power of ECS over TCR during the latter half of the 21st century in areas with slow warming, illustrating that although TCR is a better predictor of warming on a global scale, it does not capture delayed regional feedbacks, or pattern effects. The transient warming at CO₂ quadrupling (T140) is consequently found to be correlated with temperature anomaly for a longer time than TCR. T140 also best describes the pattern of regional temperature anomaly at the end of the century. These results will be of use in the continued work on emergent constraints on climate sensitivity, as a guide to what measure of sensitivity is actually the most meaningful to constrain, depending on the time period in focus. The findings are summarized in Huusko et al. (2021).

Task 6.2: Develop new metrics for ESM evaluation with the goal of “getting the right answer for the right reason”

In a step towards new ways of evaluating, and constraining models and their cloud feedback and thereby sensitivity, Task 6.2 has partly focused on the “too-few-too-bright” problem, i.e. that models tend to produce clouds that cover less area, and are more reflective than suggested by observations, and by compensating errors arrive at a reasonable TOA radiative effect. Using a compilation of several historical satellite data sets (CLARA-2A, Cloud_cci, PATMOS-x, MODIS and CERES) we find that this bias is present for clouds over ocean across latitudes, and persists in both CMIP5 and CMIP6 models. Preliminary results indicate that models with smaller combined biases in cloud fraction, and cloud brightness, and distributions therein, are at the higher end of the sensitivity range. These results were presented at EGU 2021 (Kuma and Bender 2021).

Another part of Task 6.2 has been dedicated to optimizing the usage of network analysis, specifically the δ -Maps method, as a “workhorse” to build climate networks from aerosol-cloud interaction and climate model simulations and evaluate them using a series of network metrics. The method is complete and we have begun the evaluation of the CMIP5/CMIP6 historical runs simulated by the three FORCES ESMs in order to get the “past performance” of the simulated sea surface temperatures (SST) against the “ground truth” from reanalysis. The purpose is to quantify model biases and to characterize the internal variability of simulations, by representing different metrics of simulated and observed networks in metric spaces. Preliminary results suggest that for

some of the ESMs examined (EC-Earth) there are distinct shifts in the model dynamics between CMIP5 and CMIP6 iterations that are outside the natural variability envelope of the model. The methodology is also being improved to include causal link inferences which will be very important to understand which aspects of the climate system and teleconnections are truly causal in nature. The results were presented at EGU 2020 (Ricard et al. 2020).

Task 6.3: Re-evaluate FORCeS ESMs with respect to climate sensitivity – what are the implications for near-term climate evolution?

This Task has started only six months ago (in M18 of the project) so there is nothing published yet.

Task 6.4: Link aerosol forcing to peak warming by using statistical methods/simplified models

This Task has started only six months ago (in M18 of the project), but some first piloting studies are applying the simplified methodologies for analysing the usefulness, costs and relevant metrics for a “two-basket” approach in emission climate change mitigation – where cumulative and long-lived climate pollutants could be accounted for separately in policy discourse and global stocktake (Allen et al. 2021; Cain et al., 2021).

5.7 Scientific progress contributing to the FORCeS objectives during the first two years of the project

The three objectives specified in the DoA and in Sect. 3 above have been guiding the work within FORCeS during the first two years. Overall, significant progress has been made towards all objectives as outlined below.

Scientific progress towards Objective 1: During the first two years, FORCeS has consolidated and re-evaluated the key processes and aerosol components identified in the DoA, and progressed towards targeted improvements of these aspects within the FORCeS ESMs (see Sects. 5.1–5.3). In the case of aerosol (see Sect. 5.1), we have chosen to focus particularly on organic aerosol, aerosol nitrate, ultrafine aerosol dynamics and emissions, and absorbing aerosol. For clouds (see Sect. 5.2), the consortium is targeting all the relevant processes governing the evolution of a cloud: from the formation of cloud droplets or ice crystals to precipitation formation – including aerosol and precursor processing and scavenging by clouds. In parallel with the targeted improvements of the aforementioned processes, analysis of model sensitivities, performance and observational constraints is ongoing to help simplify the process descriptions (see Sects. 5.3 and 5.4) where possible and rule out implausible model variants. Finally, to set the scene for evaluating the FORCeS ESMs after the process improvements, we have benchmarked various aspects of these models as it was within their contribution to the CMIP6 (Climate Model Intercomparison Project phase 6) project (see Sects. 5.5 and 5.6).

Scientific progress towards Objective 2: We have analysed the budgets of key aerosol components as simulated by the FORCeS ESMs during the past decade, and started the analysis for the corresponding radiative forcing estimates and the most important factors causing uncertainty in these estimates (see Sect. 5.3). These analyses highlight e.g. the importance of understanding the factors controlling the lifetime of aerosol constituents within the ESMs. We have collected and identified the data sets to be utilized for finding new constraints for the anthropogenic aerosol forcing, and started a process of finding observational constraints for the key processes targeted that span over all the relevant scales – from the molecular to the global scale. Planning of simulation and model evaluation strategies is in an intense phase within FORCeS, including also the use of approaches that allow for multidimensional model sensitivity analysis, with the aim to maximally use the observational constraints for narrowing the plausible range of anthropogenic aerosol forcing.

Scientific progress towards Objective 3: First concrete recommendations for model improvements based on best available process-level knowledge (literature but also original new science from FORCeS) have been provided and ESM modification has started (see Sects. 5.5–5.6). Simulations and evaluation planning with the updated ESMs is ongoing. The work towards first estimates of near-term aerosol forcing using the FORCeS ESMs has started, and the features of the participating ESMs has been investigated before the planned process improvements (see Sects. 5.5–5.6) to pave the way for understanding the role of the targeted processes in governing, and potentially improving, transient climate simulations.

6. Summary and outlook

Overall, FORCeS has progressed according to the plan laid out in the DoA, with some relatively minor deviations caused primarily by the COVID-19 pandemic. Progress has been made towards understanding and reducing the uncertainty in estimates of the radiative forcing associated with anthropogenic aerosol. Specifically, we have consolidated key aerosol components (organics, nitrate, absorbing components) and processes (ultrafine aerosol dynamics, interactions with clouds) as well as cloud processes (interaction with aerosol particles, microphysics of precipitation formation, ice formation and updrafts) to target in the FORCeS Earth System Models (ESMs, i.e. EC-Earth, ECHAM/ICON and NorESM). We are in the process of updating and evaluating the descriptions of these key processes within the FORCeS ESMs based on a wealth of observational data over various scales, as well as to smaller-scale theoretical considerations, to ensure physical and chemical robustness of the climate-scale representation of these processes. We use the observational constraints together with sophisticated multidimensional analysis of the model response to narrow down the plausible range of aerosol and cloud evolution, as well as radiative forcing estimates. To fill key gaps in observational constraints, novel laboratory experiments and field campaigns are ongoing within FORCeS, and we are using detailed models to develop new and more process-based metrics and constraints for climate model evaluation.

During the first two years, FORCeS has established an active, engaged and productive researcher community that brings together experts focusing on detailed aerosol- and cloud-related processes and those working on Earth system prediction. We have established the FORCeS stakeholder group, and first communications with the key stakeholders have included the production of a policy brief addressing the dual role of aerosol particles in the potential path towards the targets of the Paris agreement and as one of the most important factors deteriorating air quality. The work within FORCeS is envisioned to progress as originally planned also during the next half of the project. Per recommendation of the Scientific Advisory Group (SAG), specific attention during this critical time will be paid to carefully planning the coordinated simulations and their evaluation, and establishment of robust observational constraints throughout the multitude of relevant scales involved.

References

FORCeS publications are marked in bold text.

- Allen, M.; Tanaka, K.; Macey, A.; Cain, M.; Jenkins, S.; Lynch, J.; Smith, M., 2021. Ensuring that offsets and other internationally transferred mitigation outcomes contribute effectively to limiting global warming. *Env. Res. Lett.*, 16, 1088/1748-9326/abfcf9**
- Allen, R. J.; Turnock, S.; Nabat, P.; Neubauer, D.; Lohmann, U.; Olivie, D.; Oshima, N.; Michou, M.; Wu, T.; Zhang, J.; Takemura, T.; Schulz, M.; Tsigaridis, K.; Bauer, S. E.; Emmons, L.; Horowitz, L.; Naik, V.; van Noije, T.; Bergman, T.; Lamarque, J.-F.; Zanis, P.; Tegen, I.; Westervelt, D. M.; Le Sager, P.; Good, P.; Shim, S.; O'Connor, F.; Akritidis, D.; Georgoulias, A. K.; Deushi, M.; Sentman, L. T.; Fujimori, S.; Collins, W. J., 2020, *Climate and air quality impacts due to mitigation of non-methane near-term climate forcers*, *Atmos. Chem. Phys.*, 20, 9641-9663, 10.5194/acp-20-9641-2020**
- Baker, A.R.; Kanakidou, M.; Nenes, A.; Myriokefalitakis, S.; Croot, P. L.; Duce, R.A.; Yuan Gao, Y.; Guieu, C; Ito, A.; Jickells, T.D.; Mahowald, M.A; Middag, R.; Perron, M.M.G.; Sarin, MM.; Shelley, R.; Turner D.R. *Changing atmospheric acidity as a modulator of nutrient deposition and ocean biogeochemistry*, 2021, *Sci. Adv.*, 7, 10.1126/sciadv.abd8800**
- Bardakov R.; Thornton, J. A.; Riipinen, I.; Krejci, R.; and Ekman, A. M. L. *Transport and chemistry of isoprene and its oxidation products in deep convective clouds*, 2021, *Tellus B*, 73, 1–21, 10.1080/16000889.2021.1979856**
- Bell, D. M.; Wu, C.; Bertrand, A.; Graham, E.; Schoonbaert, J.; Giannoukos, S.; Baltensperger, U.; Prevot, A. S. H.; Riipinen, I.; El Haddad, I.; and Mohr, C.: *Particle-phase processing of α -pinene NO₃ secondary organic aerosol in the dark*, 2021, *Atmos. Chem. Phys. Discuss.* [preprint], <https://doi.org/10.5194/acp-2021-379>, in review.
- Bond, T. C. and Bergstrom, R. W., 2006. *Light Absorption by Carbonaceous Particles: An Investigative Review*, *Aerosol Sci. Tech.*, 40, 27–67, <https://doi.org/10.1080/02786820500421521>.
- Bulatovic, I.; Igel, A. L.; Leck, C.; Heintzenberg, J.; Riipinen, I.; and Ekman, A. M. L., 2021. *The importance of Aitken mode aerosol particles for cloud sustenance in the summertime high Arctic: A simulation study supported by observational data*. *Atmos. Chem. Phys.*, 10.5194/acp-21-3871-2021**

- Cain, M.; Shine, K.; Frame, D.; Lynch, J.; Macey, A.; Pierrehumbert, R.; Allen, M. Comment on 'unintentional unfairness when applying new greenhouse gas emissions metrics at country level'. *Env. Res. Lett.*, **16**, 10.1088/1748-9326/ac02eb
- Cherian, R.; Quaas, J., 2020. Trends in AOD, clouds, and cloud radiative effects in satellite data and CMIP5 and CMIP6 model simulations over aerosol source regions. *Geophys. Res. Lett.*, **47**, e2020GL087132, <https://doi.org/10.1029/2020GL087132>.
- Christensen, M.; Gettelman, A.; Cermak, J.; Dagan, G.; Diamond, M.; Douglas, A.; Feingold, G.; Glassmeier, F.; Goren, T.; Grosvenor, D.; Gryspeerd, E.; Kahn, R.; Li, Z.; Ma, P.-L.; Malavelle, F.; McCoy, I.; McCoy, D.; McFarquhar, G.; Mülmenstädt, J.; Pal, S.; Possner, A.; Povey, A.; Quaas, J.; Rosenfeld, D.; Schmidt, A.; Schrödner, R.; Sorooshian, A.; Stier, P.; Toll, V.; Watson-Parris, D.; Wood, R.; Yang, M. and Yuan, T., 2021. Opportunistic Experiments to Constrain Aerosol Effective Radiative Forcing, *Atmos. Chem. Phys. Discuss.* [preprint], <https://doi.org/10.5194/acp-2021-559>, in review.
- Claquin, T.; Schulz, M. and Y. J. Balkanski. 1999. Modeling the Mineralogy of Atmospheric Dust Sources. *Journal of Geophysical Research Atmospheres* 104 (D18): 22243–56. <https://doi.org/10.1029/1999JD900416>.
- Collins, J. W.; Lamarque, J. F.; Schulz, M.; Boucher, O.; Eyring, V.; Hegglin, I. M.; Maycock, A. et al. 2017. *AerChemMIP: Quantifying the Effects of Chemistry and Aerosols in CMIP6*. *Geosci. Model Devel.* **10** (2): 585–607. <https://doi.org/10.5194/gmd-10-585-2017>.
- Dagan, G.; Stier, P.; Watson-Parris, D., 2020. Aerosol Forcing Masks and Delays the Formation of the North Atlantic Warming Hole by Three Decades, *Geophys. Res. Lett.*, **10.1029/2020GL090778**
- Donahue, N. M.; Robinson, A. L.; Stanier, C. O.; Pandis, S. N. Coupled Partitioning, Dilution, and Chemical Aging of Semivolatile Organics, 2006, *Environ. Sci. Technol.* **40** (8): 2635–43. <https://doi.org/10.1021/es052297c>.
- Douglas, A. and Stier, P., 2021. Using the learnings of machine learning to distill cloud controlling environmental regimes from satellite observations, *EGU General Assembly 2021, online, 19–30 Apr 2021, EGU21-16443*, <https://doi.org/10.5194/egusphere-egu21-16443>.
- Eyring, V.; Bony, S.; Meehl, G. A.; Senior, C. A.; Stevens, B.; Stouffer, R. J.; Taylor, K. E. 2016. Overview of the Coupled Model Intercomparison Project Phase 6 (CMIP6) Experimental Design and Organization. *Geosci. Model Devel.* **9** (5): 1937–58. <https://doi.org/10.5194/gmd-9-1937-2016>.
- Eyring, V.; Cox, P.M.; Flato, G.M. et al., 2019. Taking climate model evaluation to the next level. *Nature Clim Change* **9**, 102–110. <https://doi.org/10.1038/s41558-018-0355-y>
- Fiedler, S.; Wyser, K.; Rogelj, J.; van Noije, T., 2021. Radiative effects of reduced aerosol emissions during the COVID-19 pandemic and the future recovery, *Atmos. Res.*, **264**, 105866, [10.1016/j.atmosres.2021.105866](https://doi.org/10.1016/j.atmosres.2021.105866).
- Frey, L.; Höpner, F.; Kirkevåg, A.; Bender F. A. M., 2021. Absorbing aerosols over Asia – an inter-model and model-observation comparison study using CAM5.3-Oslo, *Tellus B: Chemical and Physical Meteorology*, **73:1**, 1–25, DOI: [10.1080/16000889.2021.1909815](https://doi.org/10.1080/16000889.2021.1909815)
- Fountoukis, C.; and A. Nenes. ISORROPIAII: A Computationally Efficient Thermodynamic Equilibrium Model for K^+ - Ca^{2+} - Mg^{2+} - NH_4^+ - Na^+ - SO_4^{2-} - NO_3^- - Cl^- - H_2O Aerosols, 2007. *Atmospheric Chemistry and Physics* **7** (17): 4639–59. <https://doi.org/10.5194/acp-7-4639-2007>.
- Gliß, J.; Mortier, A.; Schulz, M.; Andrews, E.; Balkanski, Y.; Bauer, S. E.; Benedictow, A. M. K.; Bian, H.; Checa-Garcia, R.; Chin, M.; Ginoux, P.; Griesfeller, J. J.; Heckel, A.; Kipling, Z.; Kirkevåg, A.; Kokkola, H.; Laj, P.; Le Sager, P.; Lund, M. T.; Lund Myhre, C.; Matsui, H.; Myhre, G.; Neubauer, D.; van Noije, T.; North, P.; Olivé, D. J. L.; Rémy, S.; Sogacheva, L.; Takemura, T.; Tsigaridis, K.; Tsyro, S. G., 2021. AeroCom phase III multi-model evaluation of the aerosol life cycle and optical properties using ground- and space-based remote sensing as well as surface in situ observations, *Atmos. Chem. Phys.*, **21**, 87–128, <https://doi.org/10.5194/acp-21-87-2021>.
- Graham, E. L.; Zieger, P.; Mohr, C.; Wideqvist, U.; Hennig, T.; Ekman, A. M. L.; Krejci, R.; Ström, J.; Riipinen, I., 2020. Physical and Chemical Properties of Aerosol Particles and Cloud Residuals on Mt. Åreskutan in Central Sweden during Summer 2014. *Tellus, Series B: Chemical and Physical Meteorology* **72** (1): 1–16. <https://doi.org/10.1080/16000889.2020.1776080>.
- Große, M. R.; Gregory, J.; Colman, R.; Andrews, T., 2018. What climate sensitivity index is most useful for projections? *Geophys. Res. Lett.*, **45**, 1559–1566. <https://doi.org/10.1002/2017GL075742>.
- Gryspeerd, E.; Goren, T.; Smith, T. W. P. Observing the timescales of aerosol-cloud interactions in snapshot satellite images, 2021. *Atmos. Chem. Phys.*, **10.5194/acp-21-6093-2021**.
- Hasekamp, O.; Gryspeerd, E.; Quaas, J. Analysis of polarimetric satellite measurements suggests stronger cooling due to aerosol-cloud interactions, 2019. *Nat. Comms.*, **10**, 5405, [10.1038/s41467-019-13372-2](https://doi.org/10.1038/s41467-019-13372-2)

- Heikkinen, L.; Äijälä, M.; Daellenbach, K. R.; Chen, G.; Garmash, O.; Aliaga, D.; Graeffe, F.; Rätty, M.; Luoma, K.; Aalto, P.; Kulmala, M.; Petäjä, T.; Worsnop, D.; Ehn, M.: *Eight years of sub-micrometre organic aerosol composition data from the boreal forest characterized using a machine-learning approach*, *Atmos. Chem. Phys.*, **21**, 10081–10109, <https://doi.org/10.5194/acp-21-10081-2021>, 2021.
- Herbert, R.; Stier, P.; Dagan, G., 2021. *Isolating large-scale smoke impacts on cloud and precipitation processes over the Amazon with convection permitting resolution*. *J. Geophys. Res.*, **126**, e2021JD034615. <https://doi.org/10.1029/2021JD034615>.
- Holopainen, E.; Kokkola, H.; Laakso, A.; and Kühn, T. *In-cloud scavenging scheme for sectional aerosol modules – implementation in the framework of the Sectional Aerosol module for Large Scale Applications version 2.0 (SALSA2.0) global aerosol module*, 2020, *Geosci. Model Dev.*, **13**, 6215–6235, <https://doi.org/10.5194/gmd-13-6215-2020>.
- Huusko, L. L.; Bender, F. A. M.; Ekman, A. M. L.; Storelvmo, T., 2021. *Climate sensitivity indices and their relation with projected temperature change in CMIP6 models*, *Env. Res. Lett.*, **16**, 64095, [10.1088/1748-9326/ac0748](https://doi.org/10.1088/1748-9326/ac0748).
- Journet, E.; Balkanski, Y. and Harrison, S. P. 2014. "A New Data Set of Soil Mineralogy for Dust-Cycle Modeling." *Atmospheric Chemistry and Physics* **14** (8): 3801–16. <https://doi.org/10.5194/acp-14-3801-2014>.
- Kakavas, S.; Pandis, S. N. *Effects of urban dust emissions on fine and coarse PM levels and composition*, 2021, *Atmos. Environ.*, **10.1016/j.atmosenv.2020.118006**.
- Karydis, V.A.; Tsimpidi, A.P.; Pozzer, A.; Lelieveld, J. *How alkaline compounds control atmospheric aerosol particle acidity*, 2021, *Atmos. Chem. Phys.*, **21**, 14983–15001, [10.5194/acp-21-14983-2021](https://doi.org/10.5194/acp-21-14983-2021).
- Kim, M.; Cermak, J.; Andersen, H.; Fuchs, J.; Stirnberg, R., 2020. *A New Satellite-Based Retrieval of Low-Cloud Liquid-Water Path Using Machine Learning and Meteosat SEVIRI Data*, *Remote Sens.*, **10.3390/rs12213475**.
- Klose, M.; Jorba, O.; Gonçalves Ageitos, M.; Escribano, J.; Dawson, M. L.; Obiso, V.; Di Tomaso, E.; Basart, S.; Montané Pinto, G.; Macchia, F.; Ginoux, P.; Guerschman, J.; Prigent, C.; Huang, Y.; Kok, J. F.; Miller, R. L.; and Pérez García-Pando, C. 2021. *Mineral dust cycle in the Multiscale Online Nonhydrostatic Atmosphere Chemistry model (MONARCH) Version 2.0*, *Geosci. Model Dev.*, **14**, 6403–6444, <https://doi.org/10.5194/gmd-14-6403-2021>.
- Kok, J. F. 2011. *Does the Size Distribution of Mineral Dust Aerosols Depend on the Wind Speed at Emission?* *Atmos. Chem. and Phys.* **11** (19): 10149–56. <https://doi.org/10.5194/acp-11-10149-2011>.
- Kok, J. F.; Adebisi, A. A.; Albani, S.; Balkanski, Y.; Checa-Garcia, R.; Chin, M.; Colarco, P. R.; Hamilton, D. S.; Huang, Y.; Ito, A.; Klose, M.; Li, L.; Mahowald, N. M.; Miller, R. L.; Obiso, V.; Pérez García-Pando, C.; Rocha-Lima, A. and Wan, J. S. 2021a. *Contribution of the world's main dust source regions to the global cycle of desert dust*, *Atmos. Chem. Phys.*, **21**, 8169–8193, <https://doi.org/10.5194/acp-21-8169-2021>.
- Kok, J. F.; Adebisi, A. A.; Albani, S.; Balkanski, Y.; Checa-Garcia, R.; Chin, M.; Colarco, P.R.; Hamilton, D.S.; Huang, Y.; Ito, A.; Klose, M.; Leung, D.M.; Li, L.; Mahowald, N.M.; Miller, R.L.; Obiso, V.; Pérez García-Pando, C.; Rocha-Lima, A.; Wan, J.S. and Whicker, C.A. 2021b. *Improved representation of the global dust cycle using observational constraints on dust properties and abundance*, *Atmos. Chem. Phys.*, **21**, 8127–8167, [10.5194/acp-21-8127-2021](https://doi.org/10.5194/acp-21-8127-2021).
- Krishnan, S.; Ekman, A. M. L.; Hansson, H.-C.; Riipinen, I.; Lewinschal, A.; Wilcox, L. J.; Dall'ajof, T., 2020. *The roles of the atmosphere and ocean in driving Arctic warming due to European aerosol reductions*. *Geophys. Res. Lett.*, **47**, e2019GL086681. <https://doi.org/10.1029/2019GL086681>
- Kuma, P.; Bender, F. *Climate sensitivity and the Southern Ocean: the effect of the "too few, too bright" model cloud problem*, *EGU General Assembly 2021*, online, 19–30 Apr 2021, EGU21-14733, <https://doi.org/10.5194/egusphere-egu21-14733>, 2021.
- Laaksonen, A.; Malila, J.; and Nenes, A.: *Heterogeneous nucleation of water vapor on different types of black carbon particles*, 2020. *Atmos. Chem. Phys.*, **20**, 13579–13589, <https://doi.org/10.5194/acp-20-13579-2020>.
- Langton, T.; Stier, P.; Watson-Parris, D.; Mulcahy, J. P., 2021. *Decomposing effective radiative forcing due to aerosol cloud interactions by global cloud regimes*. *Geophys. Res. Lett.*, **48**, e2021GL093833. <https://doi.org/10.1029/2021GL093833>
- Lee, D. S.; Fahey, D. W.; Skowron, A.; Allen, M. R.; Burkhardt, U.; Chen, Q.; Doherty, S. J.; Freeman S.; Forster, P. M.; Fuglestedt, J.; Gettelman, A.; De León, R. R.; Lim, L. L.; Lund, M. T.; Millar, R. J.; Owen, B.; Penner, J. E.; Pitari, G.; Prather, M. J.; Sausen, R.; Wilcox, L. J., 2021. *The contribution of global aviation to anthropogenic climate forcing for 2000 to 2018*. *Atmos. Environ.* (1994). **2021 Jan 1**;244:117834. doi: [10.1016/j.atmosenv.2020.117834](https://doi.org/10.1016/j.atmosenv.2020.117834). Epub 2020 Sep 3. PMID: 32895604; PMCID: PMC7468346.

- Li, L.; Mahowald, N. M.; Miller, R. L.; Pérez García-Pando, C.; Klose, M.; Hamilton, D. S.; Gonçalves Ageitos, M.; Ginoux, P.; Balkanski, Y.; Green, R. O.; Kalashnikova, O.; Kok, J. F.; Obiso, V.; Paynter, D.; and Thompson, D. R., 2021. Quantifying the range of the dust direct radiative effect due to source mineralogy uncertainty, *Atmos. Chem. Phys.*, 21, 3973–4005, <https://doi.org/10.5194/acp-21-3973-2021>.
- Lohmann, U.; Friebel, F.; Kanji, Z. A.; Mahrt, F.; Mensah, A. A. and Neubauer, D. 2020. “Future Warming Exacerbated by Aged-Soot Effect on Cloud Formation.” *Nature Geoscience* 13 (10): 674–80. <https://doi.org/10.1038/s41561-020-0631-0>.
- Maahn, M.; Goren, T.; de Boer G.; Shupe, D. M. Liquid containing clouds at the North Slope of Alaska demonstrate sensitivity to local industrial aerosol emissions, 2021. *Geophys. Res. Lett.*, 48, e2021GL094307, [10.1029/2021GL094307](https://doi.org/10.1029/2021GL094307).
- Mortier, A.; Gliš, J.; Schulz, M.; Aas, W.; Andrews, E.; Bian, H.; Chin, M.; Ginoux, P.; Hand, J.; Holben, B.; Zhang, H.; Kipling, Z.; Kirkevåg, A.; Laj, P.; Lurton, T.; Myhre, G.; Neubauer, D.; Olivé, D.; von Salzen, K.; Skeie, R. B.; Takemura, T.; and Tilmes, S., 2020. Evaluation of climate model aerosol trends with ground-based observations over the last 2 decades – an AeroCom and CMIP6 analysis, *Atmos. Chem. Phys.*, 20, 13355–13378, <https://doi.org/10.5194/acp-20-13355-2020>.
- Myriokefalitakis, S.; Bergas-Massó, E.; Gonçalves-Ageitos, M.; Pérez García-Pando, C.; van Noije, T.; Le Sager, P.; Ito, A.; Athanasopoulou, E.; Nenes, A.; Kanakidou, M.; Krol, M. C. and Gerasopoulos, E.: Multiphase processes in the EC-Earth Earth System model and their relevance to the atmospheric oxalate, sulfate, and iron cycles, 2021, *Geosci. Model Dev. Discuss.* [preprint], <https://doi.org/10.5194/gmd-2021-357>, in review.
- Nenes, A.; Pandis, S. N.; Kanakidou, M.; Russell, A. G.; Song, S.; Vasilakos, P.; and Weber, R. J.: Aerosol acidity and liquid water content regulate the dry deposition of inorganic reactive nitrogen, 2021, *Atmos. Chem. Phys.*, 21, 6023–6033, <https://doi.org/10.5194/acp-21-6023-2021>.
- Neubauer, D.; Ferrachat, S.; Siegenthaler-Le Drian, C.; Stier, P.; Partridge, D. G.; Tegen, I.; Bey, I.; Stanelle, T.; Kokkola, H.; Lohmann, U., 2019. The Global Aerosol-Climate Model ECHAM6.3-HAM2.3-Part 2: Cloud Evaluation, Aerosol Radiative Forcing, and Climate Sensitivity, 2019. *Geosci. Model Devel.* 12 (8): 3609–39. <https://doi.org/10.5194/gmd-12-3609-2019>.
- Nickovic, S.; Vukovic A.; Vujadinovic, M.; Djurdjevic, V. and G. Pejanovic. 2012. Technical Note: High-Resolution Mineralogical Database of Dust-Productive Soils for Atmospheric Dust Modeling. *Atmospheric Chemistry and Physics* 12 (2): 845–55. <https://doi.org/10.5194/acp-12-845-2012>.
- Onsum Moseid, K.; Schulz, M.; Storelmo, T.; Julsrud, I. R.; Olivé, D.; Nabat, P.; Wild, M. et al. 2020. “Bias in CMIP6 Models as Compared to Observed Regional Dimming and Brightening.” *Atmos. Chem. Phys.* 20 (24): 16023–40. <https://doi.org/10.5194/acp-20-16023-2020>.
- Osborne, S. R.; Johnson, B. T.; Haywood, J. M.; Baran, A. J.; Harrison, M. A. J. and McConnell, C. L., 2008. Physical and optical properties of mineral dust aerosol during the Dust and Biomass-burning Experiment, *J. Geophys. Res.*, 113, D00C03, <https://doi.org/10.1029/2007JD009551>.
- Paglione, M.; Decesari, S.; Rinaldi, M.; Tarozzi, L.; Manarini, F.; Gilardoni, S.; Facchini, M. C.; Fuzzi, S.; Bacco, D.; Trentini, A.; Pandis, S. N.; Nenes, A. Historical Changes in Seasonal Aerosol Acidity in the Po Valley (Italy) as Inferred from Fog Water and Aerosol Measurements, 2021, *Environ. Sci. Technol.* 55 (11), 7307-7315, DOI: [10.1021/acs.est.1c00651](https://doi.org/10.1021/acs.est.1c00651)
- Pasquier, J. T.; David, R. O.; Freitas, G.; Gierens, R.; Gramlich, Y.; Haslett, S.; Li, G.; Schäfer, B.; Siegel, K.; Wieder, J.; Adachi, K.; Belosi, F.; Carlsen, T.; Decesari, S.; Ebell, K.; Gilardoni, S.; Gysel-Beer, M.; Henneberger, J.; Inoue, J.; Kanji, Z. A.; Koike, M.; Kondo, Y.; Krejci, R.; Lohmann, U.; Maturilli, M.; Mazzolla, M.; Modini, R.; Mohr, C.; Motos, G.; Nenes, A.; Nicosia, A.; Ohata, S.; Paglione, M.; Park, S.; Pileci, R.; Ramelli, F.; Rinaldi, M.; Ritter, C.; Sato, K.; Storelmo, T.; Tobo, Y.; Viola, A.; Zieger, P. The Ny-Ålesund Aerosol Cloud Experiment (NASCENT): Overview and First Results, Submitted (*BAMS The Bulletin of the American Meteorological Society*), 2021
- Pérez, C.; Haustein, K.; Janjic, Z.; Jorba, O.; Huneus, N.; Baldasano, J. M.; Black, T.; Basart, S.; Nickovic, S.; Miller, R. L.; Perlwitz, J. P.; Schulz, M., and Thomson, M.: Atmospheric dust modeling from meso to global scales with the online NMMB/BSCDust model; Part 1: Model description, annual simulations and evaluation, 2011, *Atmos. Chem. Phys.*, 11, 13 001–13 027, <https://doi.org/10.5194/acp-11-13001-2011>.
- Perlwitz, J. P.; Pérez García-Pando, C.; and Miller, R. L.: Predicting the mineral composition of dust aerosols – Part 1: Representing key processes, 2015a, *Atmos. Chem. and Phys.*, 15, 11 593–11 627, <https://doi.org/10.5194/acp-15-11593-2015>

- Perlwitz, J. P.; Pérez García-Pando, C.; and Miller, R. L.: Predicting the mineral composition of dust aerosols – Part 2: Model evaluation and identification of key processes with observations, *Atmos. Chem. Phys.*, 15, 11 629–11 652, <https://doi.org/10.5194/acp15-11629-2015>, 2015b.
- Proske, U.; Bessenbacher, V.; Dedekind, Z.; Lohmann, U.; Neubauer, D. How frequent is natural cloud seeding from ice cloud layers ($< -35\text{ }^{\circ}\text{C}$) over Switzerland? 2021. *Atmos. Chem. Phys.*, 10.5194/acp-21-5195-2021.
- Quaas, J.; Antti A.; Cairns, B.; Christensen, M.; Deneke, H.; Ekman, A. M. L.; Feingold, G. et al. 2020. “Constraining the Twomey Effect from Satellite Observations: Issues and Perspectives.” *Atmos. Chem. Phys.* 20: 15079–99. <https://doi.org/10.5194/acp-20-15079-2020>.
- Quaas, J.; Gryspeerdt, E.; Vautard, R.; Boucher, O., 2021. Climate impact of aircraft-induced cirrus assessed from satellite observations before and during COVID-19. *Env. Res. Lett.*, 16, 64051, 10.1088/1748-9326/abf686
- Ricard, L.; Nenes, A.; Runge, J.; Georgakaki, P.: Exploring microphysical properties of marine boundary layer clouds through network analysis, *EGU General Assembly 2021*, online, 19–30 Apr 2021, EGU21-13307, <https://doi.org/10.5194/egusphere-egu21-13307>, 2021.
- Rinaldi, M.; Hiranuma, N.; Santachiara, G.; Mazzola, M.; Mansour, K.; Paglione, M.; Rodriguez, C. A.; Traversi, R.; Becagli, S.; Cappelletti, D. and Belosi, F., 2021. Ice-nucleating particle concentration measurements from Ny-Ålesund during the Arctic spring–summer in 2018, *Atmos. Chem. Phys.*, 21, 14725-14748, 10.5194/acp-21-14725-2021
- Ruuskanen, A.; Romakkaniemi, S.; Kokkola, H.; Arola, A.; Mikkonen, S.; Portin, H.; Virtanen, A.; Lehtinen, K. E. J.; Komppula, M. and Leskinen, A., 2021. Observations on aerosol optical properties and scavenging during cloud events, *Atmos. Chem. Phys.*, 21, 1683–1695, <https://doi.org/10.5194/acp-21-1683-2021>.
- Samset, B. H.; Stjern, C. W.; Andrews, E.; Kahn, R. A.; Myhre, G.; Schulz, M. and Schuster, G. L., 2018. Aerosol Absorption: Progress Towards Global and Regional Constraints, *Current Climate Change Reports*, 4, 65–83, <https://doi.org/10.1007/s40641-018-0091-4>.
- Sand, M.; Samset, B. H.; Myhre, G.; Gliß, J.; Bauer, S. E.; Bian, H.; Chin, M.; Checa-Garcia, R.; Ginoux, P.; Kipling, Z.; Kirkevåg, A.; Kokkola, H.; Le Sager, P.; Lund, M. T.; Matsui, H.; van Noije, T.; Olivié, D. J. L.; Remy, S.; Schulz, M.; Stier, P.; Stjern, C. W.; Takemura, T.; Tsigaridis, K.; Tsyro, S. G. and Watson-Parris, D.: Aerosol absorption in global models from AeroCom phase III, *Atmos. Chem. Phys.*, 21, 15929–15947, <https://doi.org/10.5194/acp-21-15929-2021>, 2021.
- Schlund, M.; Lauer, A.; Gentine, P.; Sherwood, S. C.; Eyring, V., 2020, Emergent constraints on equilibrium climate sensitivity in CMIP5: do they hold for CMIP6?, *Earth Syst. Dynam.*, 11, 1233–1258, <https://doi.org/10.5194/esd-11-1233-2020>
- Seland, Ø.; Bentsen, M.; Olivié, D.; Toniazzo, T.; Gjermundsen, A.; Seland Graff, L.; Boldingh Debernard, J. et al. 2020. Overview of the Norwegian Earth System Model (NorESM2) and Key Climate Response of CMIP6 DECK, Historical, and Scenario Simulations, 2020. *Geosci. Model Devel.* 13 (12): 6165–6200. <https://doi.org/10.5194/gmd-13-6165-2020>.
- Schlesinger, D.; Riipinen, I.; Lowe, S. J.; Olenius, T.; Kong, X. and Pettersson, J. B. C. 2020. Molecular Perspective on Water Vapor Accommodation into Ice and Its Dependence on Temperature. *J. Phys. Chem. A* 124 (51): 10879–89. <https://doi.org/10.1021/acs.jpca.0c09357>.
- Schmale, J.; Zieger, P.; Ekman, A. M. L. Aerosols in current and future Arctic climate, 2021, *Nature Clim. Change*, 10.1038/s41558-020-00969-5
- Siegel, K.; Karlsson, L.; Zieger, P.; Baccharini, A.; Schmale, J.; Lawler, M.; Salter, M.; Leck, C.; Ekman, A. M. L.; Riipinen, I.; Mohr, C. Insights into the molecular composition of semi-volatile aerosols in the summertime central Arctic Ocean using FIGAERO-CIMS, 2021, *Environ. Sci.: Atmos.*, 10.1039/d0ea00023j
- Spill, G.; Stier, P.; Field, P. R.; Dagan, G. Contrasting responses of idealised and realistic simulations of shallow cumuli to aerosol perturbations, 2021. *Geophys. Res. Lett.*, 48, e2021GL094137, 10.1029/2021GL094137
- Sotiropoulou, G.; Ickes, L.; Nenes, A.; Ekman, A. M. L. Ice multiplication from ice-ice collisions in the high Arctic: sensitivity to ice habit, rimed fraction, ice type and uncertainties in the numerical description of the process, 2021a. *Atmos. Chem. Phys.*, 21, 9741--9760, 10.5194/acp-21-9741-2021.
- Sotiropoulou, G.; Vignon, É.; Young, G.; Morrison, H.; O’Shea, S. J.; Lachlan-Cope, T.; Berne, A., and Nenes, A. Secondary ice production in summer clouds over the Antarctic coast: an underappreciated process in atmospheric models, 2021b. *Atmos. Chem. Phys.*, 21, 755–771, <https://doi.org/10.5194/acp-21-755-2021>.

Su, W.; Liang, L.; Myhre, G.; Thorsen, T. J.; Loeb, N. G.; Schuster, G. L.; Ginoux, P.; Paulot, F.; Neubauer, D.; Checa-Garcia, R.; Matsui, H.; Tsigaridis, K.; Skeie, R. B.; Takemura, T.; Bauer, S. E.; Schulz, M. 2021, *Understanding Top-of-Atmosphere Flux Bias in the AeroCom Phase III Models: A Clear-Sky Perspective*, JAMES, 13, e2021MS002584, 10.1029/2021MS002584

Theodoritsi, G.; Ciarelli, G.; Pandis, S. N. *Simulation of the evolution of biomass burning organic aerosol with different volatility basis set schemes in PMCAMx-SR v1.0*, 2021, Geosci. Model Dev., 10.5194/gmd-14-2041-2021

Tsimpidi, A. P.; Karydis, V. A.; Pozzer, A.; Pandis, S. N.; Lelieveld, J. ORACLE (v1.0): Module to Simulate the Organic Aerosol Composition and Evolution in the Atmosphere. Geosci. Model Devel. 7 (6): 3153–72. <https://doi.org/10.5194/gmd-7-3153-2014>.

Turnock, S. T.; Allen, R. J.; Andrews, M.; Bauer, S. E.; Emmons, L.; Good, P.; Horowitz, L.; Michou, M.; Nabat, P.; Naik, V.; Neubauer, D.; O'Connor, F. M.; Olivie, D.; Schulz, M.; Sellar, A.; Takemura, T.; Tilmes, S.; Tsigaridis, K.; Wu, T.; Zhang, J., 2020. *Historical and future changes in air pollutants from CMIP6 models*, Atmos. Chem. Phys., 10.5194/acp-20-14547-2020.

van Noije, T.; Bergman, T.; Le Sager, P.; O'Donnell, D.; Makkonen, R.; Gonçalves-Ageitos, M.; Döscher, R.; Fladrich, U.; von Hardenberg, J.; Keskinen, J.-P.; Korhonen, H.; Laakso, A.; Myriokefalitakis, S.; Ollinaho, P.; Pérez García-Pando, C.; Reerink, T.; Schrödner, R.; Wyser, K.; Yang, S., 2021. *EC-Earth3-AerChem: a global climate model with interactive aerosols and atmospheric chemistry participating in CMIP6*, Geosci. Model Dev., 14, 5637–5668, <https://doi.org/10.5194/gmd-14-5637-2021>.

Villanueva, D.; Neubauer, D.; Gasparini, B.; Ickes, L.; Tegen, I. *Constraining the Impact of Dust-Driven Droplet Freezing on Climate Using Cloud-Top-Phase Observations*, 2021, Geophys. Res. Lett., 48, e2021GL092687, 10.1029/2021GL092687.

Väisänen, O.; Hao, L.; Virtanen, A.M.; Romakkaniemi, S. 2020. *Trajectory-based analysis on the source areas and transportation pathways of atmospheric particulate matter over Eastern Finland*, Tellus B, 10.1080/16000889.2020.1799687.

Wex, H.; Huang, L.; Sheesley, R.; Bossi, R.; and Traversi, R., 2019a. *Annual concentrations of ice nucleating particles at Arctic station Ny-Ålesund*, PANGAEA [data set], <https://doi.org/10.1594/PANGAEA.899696>.

Wex, H.; Huang, L.; Zhang, W.; Hung, H.; Traversi, R.; Becagli, S.; Sheesley, R. J.; Moffett, C. E.; Barrett, T. E.; Bossi, R.; Skov, H.; Hünerbein, A.; Lubitz, J.; Löffler, M.; Linke, O.; Hartmann, M.; Herenz, P. and Stratmann, F., 2019b. *Annual variability of ice-nucleating particle concentrations at different Arctic locations*, Atmos. Chem. Phys., 19, 5293–5311, <https://doi.org/10.5194/acp-19-5293-2019>.

Wu, R.; Kiendler-Scharr, A.; Wahner, A.; Hallquist, M.; Mentel, T.F. *Molecular composition and volatility of multi-generation products formed from isoprene oxidation by nitrate radical*, 2021a, Atmos. Chem. Phys., 21, 10799--10824, 10.5194/acp-21-10799-2021

Wu, C.; Bell, D. M.; Graham, E. L.; Haslett, S.; Riipinen, I.; Baltensperger, U.; Bertrand, A.; Giannoukos, S.; Schoonbaert, J.; El Haddad, I.; Prevot, A. S. H.; Huang, W. and Mohr, C.: *Photolytically induced changes in composition and volatility of biogenic secondary organic aerosol from nitrate radical oxidation during night-to-day transition*, 2021b, Atmos. Chem. Phys., 21, 14907–14925, <https://doi.org/10.5194/acp-21-14907-2021>.

Wyser K.; Kjellström E.; Koenigk T.; Martins H.; Döscher R., 2020. *Warmer climate projections in EC-Earth3-Veg: the role of changes in the greenhouse gas concentrations from CMIP5 to CMIP6*. Env. Res. Lett., 10.1088/1748-9326/ab81c2

Yli-Juuti, T.; Mielonen, T.; Heikkinen, L.; Arola, A.; Ehn, M.; Isokääntä, S.; Keskinen, H.-M.; Kulmala, M.; Laakso, A.; Lipponen, A.; Luoma, K.; Mikkonen, S.; Nieminen, T.; Paasonen, P.; Petäjä, T.; Romakkaniemi, S.; Tonttila, J.; Kokkola, H.; Virtanen, A., 2021. *Significance of the organic aerosol driven climate feedback in the boreal area*, Nat. Comms., 12, 5637, 10.1038/s41467-021-25850-7

Zhang, S.; Stier, P.; Watson-Parris, D. *On the contribution of fast and slow responses to precipitation changes caused by aerosol perturbations*, 2021. Atmos. Chem. Phys., 21, 10179--10197, 10.5194/acp-21-10179-2021.

FORCES contact information

Project manager Ana Cordeiro | ana.cordeiro@su.se
Office for Research, Engagement and Innovation Services (REIS)
Stockholm University, SE-106 91 Stockholm, Sweden